




Rapid Freezing Enables Aminoglycosides To Eradicate Bacterial Persisters via Enhancing Mechanosensitive Channel MscL-Mediated Antibiotic Uptake

Yanna Zhao,^a Boyan Lv,^a Fengqi Sun,^a Jiafeng Liu,^b Yan Wang,^a Yuanyuan Gao,^{a,c} Feng Qi,^c Zengyi Chang,^b  Xinmiao Fu^{a,c}

^aProvincial University Key Laboratory of Cellular Stress Response and Metabolic Regulation, Key Laboratory of Optoelectronic Science and Technology for Medicine of Ministry of Education, College of Life Sciences, Fujian Normal University, Fuzhou City, Fujian Province, China

^bState Key Laboratory of Protein and Plant Gene Research, School of Life Sciences, Peking University, Beijing, China

^cEngineering Research Center of Industrial Microbiology of Ministry of Education, Fujian Normal University, Fuzhou City, Fujian Province, China

Yanna Zhao, Boyan Lv, Fengqi Sun, and Jiafeng Liu contributed equally to this article. Author order was determined in order of increasing seniority.

ABSTRACT Bacterial persisters exhibit noninherited antibiotic tolerance and are linked to the recalcitrance of bacterial infections. It is very urgent but also challenging to develop antipersister strategies. Here, we report that 10-s freezing with liquid nitrogen dramatically enhances the bactericidal action of aminoglycoside antibiotics by 2 to 6 orders of magnitude against many Gram-negative pathogens, with weaker potentiation effects on Gram-positive bacteria. In particular, antibiotic-tolerant *Escherichia coli* and *Pseudomonas aeruginosa* persisters—which were prepared by treating exponential-phase cells with ampicillin, ofloxacin, the protonophore cyanide *m*-chlorophenyl hydrazone (CCCP), or bacteriostatic antibiotics—can be effectively killed. We demonstrated, as a proof of concept, that freezing potentiated the aminoglycosides' killing of *P. aeruginosa* persisters in a mouse acute skin wound model. Mechanistically, freezing dramatically increased the bacterial uptake of aminoglycosides regardless of the presence of CCCP, indicating that the effects are independent of the proton motive force (PMF). In line with these results, we found that the effects were linked to freezing-induced cell membrane damage and were attributable, at least partly, to the mechanosensitive ion channel MscL, which was able to directly mediate such freezing-enhanced aminoglycoside uptake. In view of these results, we propose that the freezing-induced aminoglycoside potentiation is achieved by freezing-induced cell membrane destabilization, which, in turn, activates the MscL channel, which is able to effectively take up aminoglycosides in a PMF-independent manner. Our work may pave the way for the development of antipersister strategies that utilize the same mechanism as freezing but do so without causing any injury to animal cells.

IMPORTANCE Antibiotics have long been used to successfully kill bacterial pathogens, but antibiotic resistance/tolerance usually has led to the failure of antibiotic therapy, and it has become a severe threat to human health. How to improve the efficacy of existing antibiotics is of importance for combating antibiotic-resistant/tolerant pathogens. Here, we report that 10-s rapid freezing with liquid nitrogen dramatically enhanced the bactericidal action of aminoglycoside antibiotics by 2 to 6 orders of magnitude against many bacterial pathogens *in vitro* and also in a mouse skin wound model. In particular, such combined treatment was able to effectively kill persister cells of *Escherichia coli* and *Pseudomonas aeruginosa*, which are *per se* tolerant of conventional treatment with bactericidal antibiotics for several hours. We also demonstrated that freezing-induced aminoglycoside potentiation was apparently linked to freezing-induced cell membrane damage that may have activated the mechanosensitive ion channel MscL, which, in turn, was able to effectively uptake

Citation Zhao Y, Lv B, Sun F, Liu J, Wang Y, Gao Y, Qi F, Chang Z, Fu X. 2020. Rapid freezing enables aminoglycosides to eradicate bacterial persisters via enhancing mechanosensitive channel MscL-mediated antibiotic uptake. *mBio* 11:e03239-19. <https://doi.org/10.1128/mBio.03239-19>.

Editor Carol A. Nancy, Sequella, Inc.

Copyright © 2020 Zhao et al. This is an open-access article distributed under the terms of the [Creative Commons Attribution 4.0 International license](https://creativecommons.org/licenses/by/4.0/).

Address correspondence to Zengyi Chang, changzy@pku.edu.cn, or Xinmiao Fu, xmfu@fjnu.edu.cn.

Received 16 December 2019

Accepted 6 January 2020

Published 11 February 2020

aminoglycoside antibiotics in a proton motive force-independent manner. Our report sheds light on the development of a new strategy against bacterial pathogens by combining existing antibiotics with a conventional physical treatment or with MscL agonists.

KEYWORDS persister, antibiotic tolerance, aminoglycoside, freezing, antibiotic uptake, MscL, mechanosensitive ion channel, cryotherapy, *Pseudomonas aeruginosa*, antibiotic resistance, drug uptake, membrane channel proteins, persistence

Curing infectious diseases caused by bacterial pathogens with antibiotics has been considered the most important medical achievement in the 20th century. However, we have also learned that bacteria are able to counteract the action of antibiotics through multiple ingenious mechanisms, including drug inactivation, alteration of drug targets, bypassing of the inhibited steps, and decreased uptake and/or increased efflux of the drug (1–3). In addition, bacteria are able to survive antibiotic attack by existing as persisters, which are genetically identical to the normal antibiotic-sensitive cells but exhibit a transient and nonheritable antibiotic tolerance (4–6). Such persister formation is widely believed to contribute to recurrent infections, as well as to the development of antibiotic resistance in pathogens (5, 7–11).

Antibiotic resistance of bacteria leads to the failure of antibiotic therapy and gives rise to life-threatening infections and has become a severe threat to global public health and economic development (12). Discovery and development of newer antibiotics have played a dominant role in this war, but as past experience indicates, resistance of pathogens to new drugs often occurs soon (12, 13). In particular, the pace of discovering new antibiotics has slowed dramatically since the 1980s, such that there has been a gap of more than 30 years since the discovery of new types of antibiotics (14, 15). This reflects both scientific and financial barriers to the identification of new antibiotics, and therefore the need to develop other strategies to fight antibiotic resistance is very urgent.

One effective strategy is to use traditional antibiotics in a wiser manner (2, 12, 14, 16, 17). In this respect, certain metabolites (e.g., glucose, mannitol, and alanine) have been reported to dramatically enhance the action of aminoglycosides against antibiotic-tolerant/resistant pathogens both *in vitro* and *in vivo* through increasing aminoglycoside uptake in a proton motive force (PMF)-dependent manner (18–22). Furthermore, inhibitors of efflux pumps have been widely reported to enhance the bactericidal action of various types of antibiotics by suppressing their outflow from bacteria (23, 24). Notably, we recently reported that hypoionic shock (i.e., treatment with ion-free solutions) could markedly potentiate aminoglycosides against *Escherichia coli* stationary-phase persisters (25). The aminoglycoside tobramycin has also been shown to be potentiated in combination with approved iron chelators (26) or the β -lactam aztreonam (27) for killing cystic fibrosis-related *Pseudomonas aeruginosa*. Other promising strategies, such as the use of membrane-active macromolecules (28), arginine-induced pH alteration (29), and osmotic compounds (30), have been reported to potentiate the existing antibiotics.

Here, we report, for the first time, that rapid freezing can dramatically and specifically enhance the bactericidal action of aminoglycoside antibiotics against normal cells and also antibiotic-tolerant persisters, both *in vitro* and in a mouse acute skin wound model. Remarkably, the aminoglycoside uptake of bacteria is enhanced by freezing in a PMF-independent manner, which is in contrast to the widely reported metabolite-stimulated aminoglycoside potentiation (18–21). The precise molecular mechanisms underlying such unusual potentiation remain unclear at present; our data indicate that the potentiation is linked to freezing-induced cell membrane damage and the MscL ion channel. Our observations pave the way for the development of promising strategies for persister eradication.

RESULTS

Freezing dramatically enhances the bactericidal action of aminoglycosides against both stationary-phase and exponential-phase *E. coli* cells. We previously

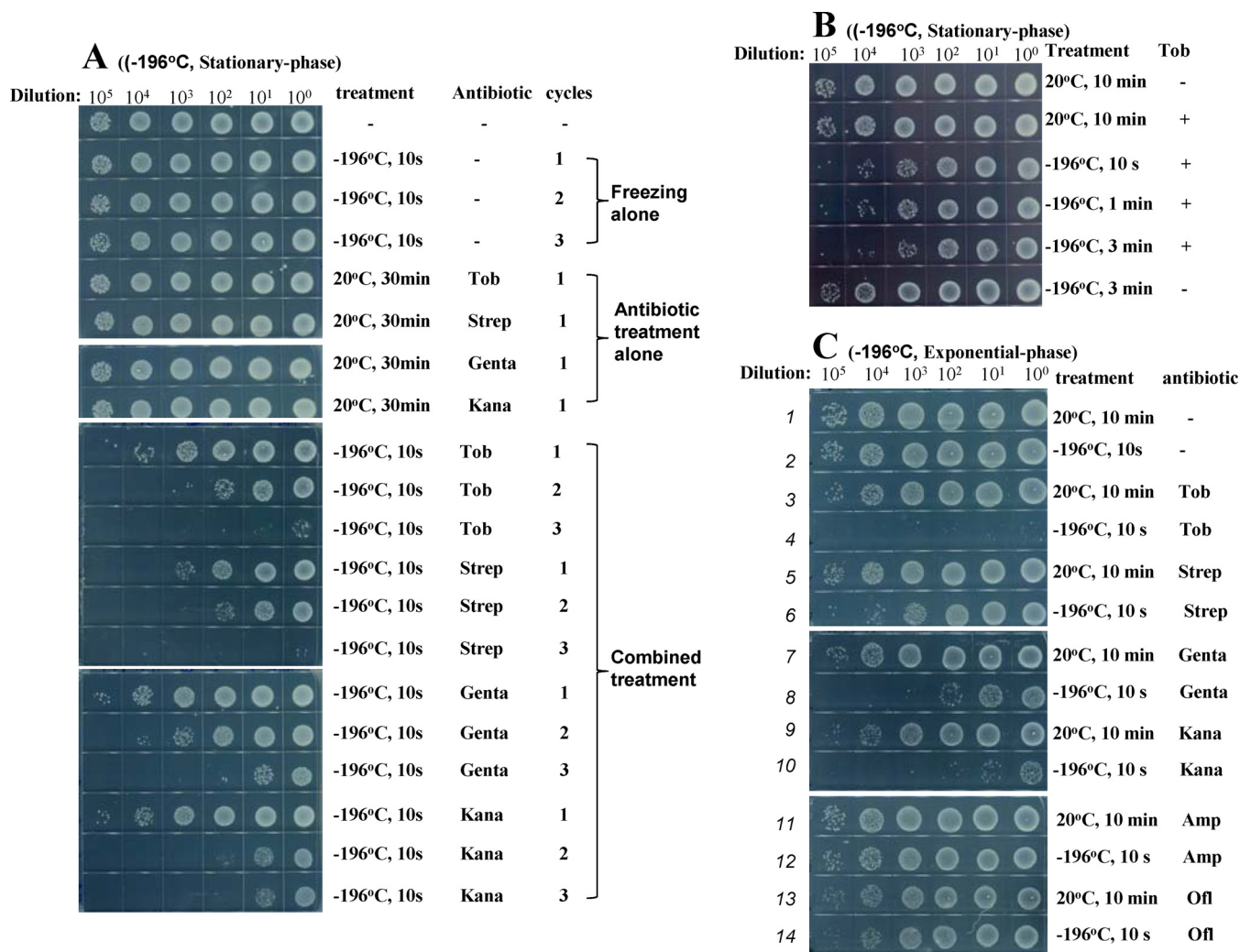


FIG 1 Freezing enhances the bactericidal action of aminoglycosides against both stationary-phase and exponential-phase *E. coli* cells. (A) Survival of *E. coli* stationary-phase cells following a 10-s treatment consisting of freezing in liquid nitrogen plus indicated aminoglycosides, with the treatment being cycled one, two, or three times. (B) Survival of *E. coli* stationary-phase cells following 10-s, 1-min, or 3-min treatment of freezing plus tobramycin. (C) Survival of *E. coli* exponential-phase cells following 10-s treatment of freezing plus indicated antibiotics. Tob, tobramycin; Strep, streptomycin; Genta, gentamicin; Kana, kanamycin; Amp, ampicillin; Ofi, ofloxacin. The treatment concentrations of the antibiotics are described in Table S1B.

reported that application of hypoionic shock for only 1 min was able to enhance the bactericidal efficacy of aminoglycoside antibiotics against *E. coli* stationary-phase cells by 4 to 5 orders of magnitude (25). We explored other physical strategies (e.g., UV exposure, sonication, microwave exposure, and freezing) for aminoglycoside potentiation. In those experiments, we found that freezing was able to significantly enhance the efficacy of aminoglycoside antibiotics (including tobramycin, streptomycin, gentamicin, and kanamycin) in killing *E. coli* cells, while other treatments were found to have severe side effects and/or little synergistic effect with aminoglycosides (data not shown).

First, we noticed that stationary-phase *E. coli* cells showed significantly reduced viability after the aminoglycoside-containing bacterial cultures were frozen in liquid nitrogen (-196°C; Fig. 1A) for 10 s or in ethanol prechilled at -80°C (see Fig. S1A in the supplemental material) for 20 s and subsequently thawed in an ice-water bath. When such combined treatments were repeated two or three times, cell viability was further reduced (Fig. 1A; see also Fig. S1A). Notably, such potentiation by freezing appears to be specific for aminoglycosides, without influencing two other classes of bactericidal antibiotics, i.e., β -lactams (ampicillin and carbenicillin) and fluoroquinolones (ofloxacin

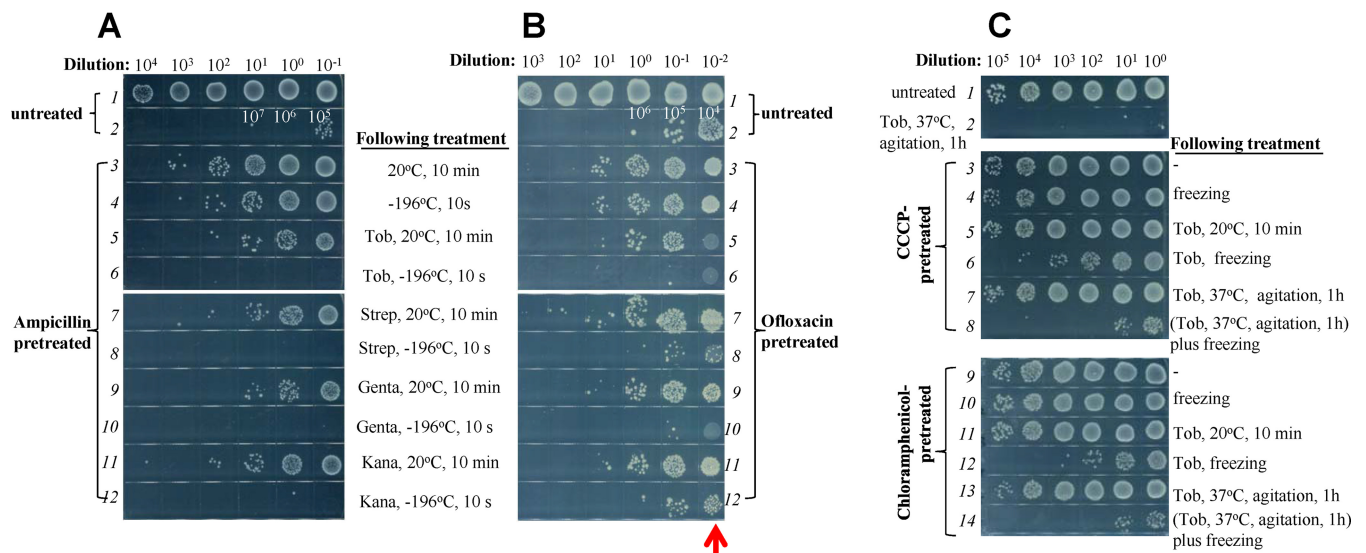


FIG 2 Freezing facilitates activity of aminoglycosides to effectively kill antibiotic-tolerant *E. coli* persisters or persister-like cells in a PMF-independent manner. (A and B) Survival of *E. coli* persister cells following a 10-s treatment consisting of freezing plus addition of the indicated aminoglycosides. Persister cells were prepared by pretreating exponential-phase cultures of *E. coli* with 100 $\mu\text{g}/\text{ml}$ ampicillin (A) or 5 $\mu\text{g}/\text{ml}$ ofloxacin (B) at 37°C for 3 h, and the remaining persister cells were concentrated 10-fold (i.e., a dilution of 10^{-1}) (A) or 100-fold (i.e., a dilution of 10^{-2}) (B) before being subjected to the combined treatment. Note that ofloxacin-treated cells, after 100-fold concentration, are extremely high in cell density and thus visible after spot plating (red arrow in panel B; see also Fig. S2A). (C) Survival of *E. coli* persister-like cells following 10-s treatment of freezing plus tobramycin. Persister-like cells were prepared by pretreating exponential-phase *E. coli* cells with 20 μM CCCP or 35 $\mu\text{g}/\text{ml}$ chloramphenicol at 37°C for 1 h and then subjected to the combined treatment with tobramycin (25 $\mu\text{g}/\text{ml}$) and freezing (lines 6 and 12). Pretreated cells were also mixed with tobramycin and agitated at 37°C for 1 h (lines 7 and 13) before freezing (lines 8 and 14).

and ciprofloxacin (Fig. S1B). Neither repeated freezing nor antibiotic treatment alone for 30 min at room temperature significantly killed the cells (Fig. 1A, top panel; see also Fig. S1A). In addition, extension of the duration of the combined treatment of tobramycin and freezing from 10 s to 3 min did not further reduce bacterial viability (Fig. 1B; see also Fig. S1C), implying that the molecular events accounting for such aminoglycoside potentiation take place during cooling and/or warming rather than during the frozen state.

In further support of the aminoglycoside potentiation by freezing, stationary-phase *E. coli* cells largely survived after a 3-h treatment with aminoglycoside at 37°C (Fig. S1D, line 1 versus line 2 [except for streptomycin]); however, these surviving cells were effectively killed upon subsequent cycled freezing (Fig. S1D, line 2 versus lines 3 to 5). We also found that freezing performed only once, either at -196°C (Fig. 1C) or at -80°C (Fig. S1E), was able to dramatically enhance the bactericidal action of aminoglycosides against exponential-phase *E. coli* cells (lines 4, 6, 8, and 10 in Fig. 1C; see also Fig. S1E). Freezing alone (lines 2 in Fig. 1C; see also Fig. S1E) or antibiotic treatment alone for 10 min at 20°C (lines 3, 5, 7, and 9 in Fig. 1C; see also Fig. S1E) did not kill the bacterial cells at significant levels. Similarly, such potentiation by freezing is specific for aminoglycosides but not for β -lactams (ampicillin) or fluoroquinolones (ofloxacin) (lines 12 and 14 in Fig. 1C; see also Fig. S1E).

Freezing enables aminoglycosides to eradicate antibiotic-tolerant *E. coli* persisters or persister-like cells in a PMF-independent manner. Bacterial persisters are widely believed to account for recurrent infections and antibiotic resistance development (5, 7–9, 31), and their eradication is of particular clinical interest. We prepared antibiotic-tolerant persister cells by treating exponential-phase cells with bactericidal antibiotics (represented by ampicillin and ofloxacin) according to earlier reports (32–34) and examined whether freezing can enhance the bactericidal effects of aminoglycosides on these persister cells. As expected, exponential-phase *E. coli* cells were mostly killed by ampicillin, with a small fraction (around 1/1,000) of original cells being ampicillin tolerant (line 3, Fig. 2A). These ampicillin-tolerant persister cells were fully eradicated by a combined treatment consisting of freezing and aminoglycoside (line 3

versus lines 6, 8, 10, and 12 in Fig. 2A) but showed only a marginal degree of killing by single treatments (line 3 versus lines 5, 7, 9, and 11). Similarly, a small fraction (around 1/1,000 to 1/10,000 of the total) of the *E. coli* exponential-phase cells were ofloxacin tolerant (line 3 in Fig. 2B), consistent with an earlier report (32), and these persisters were also effectively eradicated by the combined treatment (lines 6, 8, 10, and 12) but not by single treatments (lines 5, 7, 9, and 11).

Furthermore, we demonstrated that freezing also facilitates the killing by aminoglycosides of persister-like bacterial cells that were formed by chemical induction of antibiotic-sensitive cells. *E. coli* exponential-phase cells, initially highly sensitive to tobramycin (line 1 versus line 2 in Fig. 2C), become relatively tolerant to tobramycin (line 7) after pretreatment with the widely used protonophore carbonyl cyanide *m*-chlorophenyl hydrazone (CCCP) (35, 36). This reflects the fact that the aminoglycoside uptake by bacteria under conventional treatment conditions depends on the PMF, which can be dissipated by CCCP (18, 37, 38). Such persister-like cells, however, were effectively killed by a combined treatment consisting of addition of tobramycin and freezing (lines 6 and 8 in Fig. 2C) but not by single treatments (lines 3 and 4). We confirmed that CCCP pretreatment did decrease the PMF of *E. coli* cells as monitored by membrane potential probe-based flow cytometric analysis, and we observed that freezing itself partially impaired the PMF (Fig. S2B). Furthermore, pretreatment with FCCP (carbonyl cyanide-*p*-trifluoromethoxyphenylhydrazone; a functional analog of CCCP for PMF dissipation) was also able to suppress the bactericidal actions of tobramycin under conventional treatment conditions (line 7 versus line 2 in Fig. S2C) but did not suppress the freezing-induced tobramycin potentiation (lines 6 and 8). In view of these results, we conclude that the PMF is dispensable for the freezing-induced aminoglycoside potentiation. In further support of this notion, pretreatment with sodium azide, a widely used electron transport inhibitor, also enabled the exponential-phase *E. coli* cells to become tobramycin tolerant (line 7 versus line 2 in Fig. S2D), consistent with earlier studies (as reviewed in reference 38), and such persister-like cells were effectively killed by the combined treatment (lines 6 and 8) but not by single treatments (lines 4 and 5). We also confirmed that the intracellular ATP levels of *E. coli* exponential-phase cells were dramatically reduced after pretreatment with CCCP or sodium azide (Fig. S2E).

In addition, we observed that pretreatment of *E. coli* exponential-phase cells with bacteriostatic antibiotics such as chloramphenicol, erythromycin, and rifampin also increased the ratio of cells tolerant to tobramycin (line 13 in Fig. 2C; lines 5 and 11 in Fig. S2F), in line with earlier reports (35, 39). Again, such persister-like cells were effectively killed by the combined treatment consisting of tobramycin and freezing (lines 12 and 14 in Fig. 2C; lines 4, 6, 10, and 12 in Fig. S2F) but not by single treatments (lines 10 and 11 in Fig. 2C; lines 2, 3, 8, and 9 in Fig. S2F). Together, these observations demonstrate that freezing facilitates the killing by aminoglycoside antibiotics of not only antibiotic-sensitive cells but also antibiotic-tolerant persister and persister-like cells.

Freezing dramatically enhances the aminoglycoside uptake of *E. coli* cells in a PMF-independent manner. Prompted by earlier reports (18, 19, 22) revealing that metabolite-induced aminoglycoside potentiation is achieved by enhancing aminoglycoside uptake, we examined whether freezing could enhance the aminoglycoside uptake of *E. coli* cells via two independent methods. First, we applied a radioactivity assay as conventionally performed (38). Specifically, ³H-labeled tobramycin was mixed thoroughly with *E. coli* exponential-phase cells and then subjected to either freezing at -196°C for 10 s or continuous incubation at room temperature for 10 min. Results show that the freezing treatment enabled the cells to accumulate ³H-labeled tobramycin at a density of $4.07 \pm 0.20 \mu\text{g tobramycin}/10^9$ cells, about 5-fold higher than that of cells incubated at room temperature ($0.84 \pm 0.02 \mu\text{g tobramycin}/10^9$ cells; Fig. 3A).

Second, taking advantage of the high thermal stability of tobramycin (Fig. S3A) and the irreversible nature of aminoglycoside uptake by *E. coli* cells (40), we explored an alternative method for measuring tobramycin uptake as recently reported (41). Data

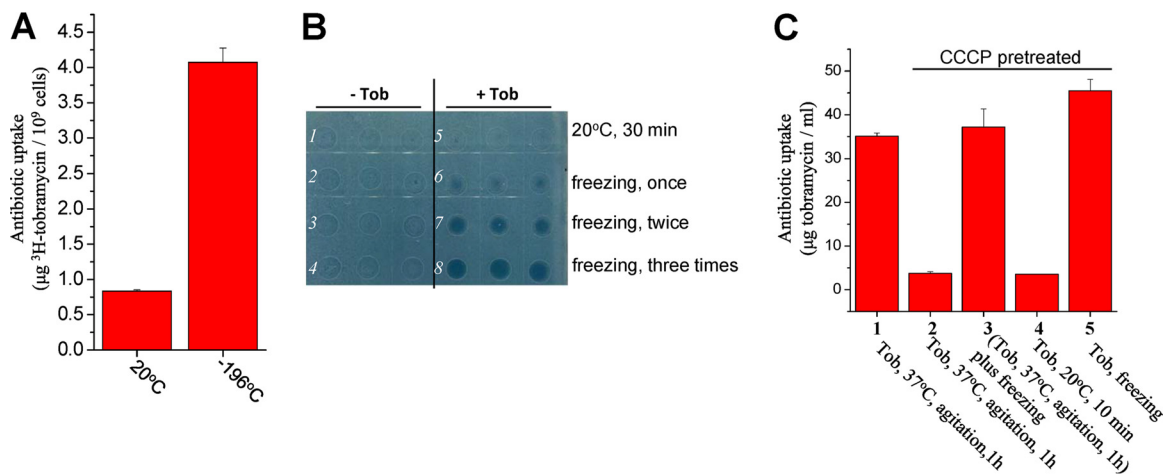


FIG 3 Freezing enhances the tobramycin uptake of *E. coli* cells in a PMF-independent manner. (A) Level of ^3H -labeled tobramycin as taken up by *E. coli* exponential-phase cells following a 10-s treatment consisting of freezing in liquid nitrogen plus addition of ^3H -labeled tobramycin (for details, see Materials and Methods). (B) Growth inhibition of *E. coli* cells on LB agar dishes by tobramycin, which was extracted from *E. coli* stationary-phase cells pretreated with tobramycin, and freezing in liquid nitrogen one, two, or three times. The procedure for tobramycin extraction was described in our earlier report (41). (C) Quantification of tobramycin taken up by CCCP-pretreated *E. coli* exponential-phase cells. Cells were treated as described for Fig. 2C and then subjected to tobramycin extraction. Quantification was performed based on the cell growth inhibition represented in Fig. S3C and the standard curve displayed in Fig. S3D. Data in panels A and C represent means \pm SD of results from three replicates.

presented in Fig. 3B indicate that tobramycin, as extracted from frozen *E. coli* stationary-phase cells, significantly inhibited bacterial growth (line 6 versus line 2), with the inhibition being stronger with more cycles of freezing (lines 6 to 8). In contrast, no significant inhibition of cell growth was observed for the tobramycin extracted from *E. coli* cells without the freezing treatment (line 5, Fig. 3B).

Furthermore, we demonstrated that freezing could enhance the tobramycin uptake of exponential-phase *E. coli* cells in a PMF-independent manner based on the following observations. First, the exponential-phase *E. coli* cells were able to effectively take up tobramycin after agitation at 37°C for 1 h (column 1 in Fig. 3C), in agreement with their high susceptibility to tobramycin (line 2 in Fig. 2C). Second, CCCP pretreatment, however, abolished this tobramycin uptake (column 2 in Fig. 3C), consistent with the fact that the PMF-dependent aminoglycoside uptake can be disrupted by CCCP (18, 37, 38). Third, when such CCCP-pretreated *E. coli* cells were agitated with tobramycin at 37°C for 1 h and then subjected to freezing, the tobramycin uptake was fully recovered (column 3 in Fig. 3C). Last, the tobramycin uptake was minimal when the CCCP-pretreated cells were incubated with tobramycin at room temperature for 10 min (column 4 in Fig. 3C) but was dramatically increased upon freezing (column 5 in Fig. 3C). These observations, together with the results indicating that freezing itself partially impaired the PMF (Fig. S2B), indicate that the PMF is dispensable for the freezing-enhanced uptake of tobramycin.

In addition, we also observed that pretreatment with chloramphenicol significantly decreased the tobramycin uptake of exponential-phase *E. coli* cells under conventional treatment conditions (column 2 versus column 1 in Fig. S3E). Nevertheless, an additional freezing treatment was able to fully recover the capacity of the cells to take up tobramycin (column 3 in Fig. S3E). Direct freezing of the chloramphenicol-pretreated cells also dramatically increased the tobramycin uptake (column 5 versus column 4 in Fig. S3E). These results agree well with the aforementioned cell survival assay results (Fig. 2C), indicating that protein synthesis is not a prerequisite for the freezing-enhanced aminoglycoside uptake, a scenario opposite that seen in the conventional aminoglycoside treatment (38).

Freezing facilitates killing of many strains of Gram-negative bacteria by aminoglycosides, with weaker effects on Gram-positive bacteria. To explore the clinical potential of the combined treatments of aminoglycosides and freezing, we examined

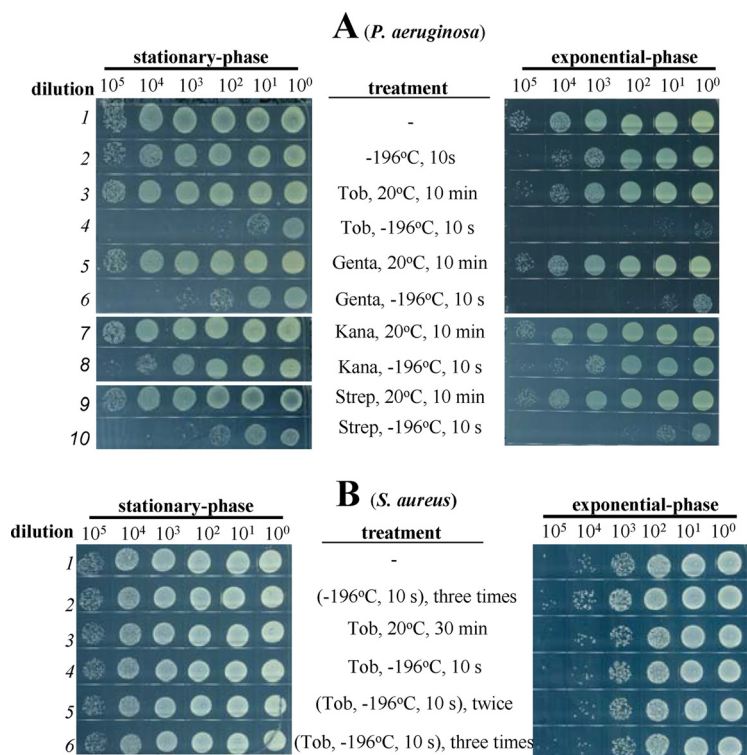


FIG 4 Freezing facilitates aminoglycoside killing of *P. aeruginosa* cells but not *S. aureus* cells. (A and B) Survival of stationary-phase (left) and exponential-phase (right) *P. aeruginosa* cells (A) and *S. aureus* cells (B) following a 10-s treatment consisting of freezing in liquid nitrogen plus addition of the indicated antibiotics at the concentrations described in Table S1B. Stationary-phase *P. aeruginosa* was frozen only once.

whether typical bacterial pathogens, such as the Gram-negative bacterium *P. aeruginosa* and the Gram-positive bacterium *Staphylococcus aureus*, could be killed. Results (Fig. 4A) indicate that both stationary-phase and exponential-phase *P. aeruginosa* cells are highly sensitive to the combined treatments (lines 4, 6, and 10) but not to tobramycin, gentamicin, or streptomycin treatment alone at room temperature (lines 3, 6, and 9). Again, freezing was unable to enhance the bactericidal action of β -lactams (ampicillin and carbenicillin) and fluoroquinolone (ofloxacin and ciprofloxacin) against *P. aeruginosa* cells (Fig. S4A). Freezing enhanced the action of kanamycin only minimally (line 8, Fig. 4A), presumably due to the intrinsic resistance of *P. aeruginosa* cells to kanamycin (left part in Fig. S4B). In contrast to *P. aeruginosa*, neither stationary-phase nor exponential-phase *S. aureus* cells were found to be sensitive to the combined treatment consisting of aminoglycoside (tobramycin) and freezing (lines 4, 5, and 6 in Fig. 4B), although exponential-phase *S. aureus* cells *per se* were sensitive to tobramycin under conventional treatment conditions (Fig. S4B).

We then expanded our test to many other Gram-negative and Gram-positive bacteria in both exponential-phase and stationary-phase states. The levels of sensitivity of these bacteria to the four types of aminoglycoside antibiotics are shown in Fig. S4C. Results of analysis of five more Gram-negative bacteria (Fig. S5A) indicate that (i) *Acinetobacter baumannii* Ab6 and *Klebsiella pneumoniae* KP-D367 are insensitive, presumably because they are resistant to these aminoglycoside antibiotics *per se* (Fig. S4C), and (ii) *Shigella flexneri* 24T7T and *Salmonella enterica* serovar Typhimurium SL1344 are sensitive to the combined treatments consisting of certain aminoglycosides and freezing in their exponential-phase and/or stationary-phase states.

Results of analysis of five more Gram-positive bacterial species (Fig. S5B) indicate that (i) *Lactococcus lactis* NZ9000 and *Enterococcus faecalis* ATCC 29212 are insensitive, presumably because they are resistant to these aminoglycoside antibiotics *per se*

TABLE 1 Sensitivity of various bacterial strains to combined aminoglycoside and freezing treatment

Bacterial species	Sensitivity to particular antibiotics ^a							
	Tom		Genta		Strep		Kana	
	A	C	A	C	A	C	A	C
<i>Escherichia coli</i>	++	+++ / ++++	++	++ / +++	++	++ / ++++	++	++ / +++
<i>Pseudomonas aeruginosa</i>	++	++ / +++	++	++ / +++	++	++ / +++	–	– / –
<i>Acinetobacter baumannii</i>	–	– / –	–	– / –	–	– / –	–	– / –
<i>Klebsiella pneumoniae</i>	–	– / –	–	– / –	–	– / –	–	– / –
<i>Salmonella enterica</i> serovar Typhimurium	++	++ / –	++	++ / –	–	– / –	++	++ / –
<i>Shigella flexneri</i>	++	++ / +++	++	– / +++	–	– / –	++	++ / +++
<i>Staphylococcus aureus</i>	++	– / –	+	– / –	–	– / –	+	– / –
<i>Lactococcus lactis</i>	–	– / –	–	– / –	–	– / –	–	– / –
<i>Enterococcus faecalis</i>	–	– / –	–	– / –	– /	– / –	–	– / –
<i>Bacillus subtilis</i>	++	+/–	++	+/–	++	+/–	++	+/–
<i>Staphylococcus epidermidis</i>	++	– / +	+	– / –	–	– / +	+	– / +
<i>Micrococcus luteus</i>	–	– / –	++	– / –	++	– / –	–	– / –

^aA, antibiotic sensitivity of each bacterium under conditions of agitation of cells in the exponential-phase state at 37°C for 1 h (for *P. aeruginosa* and *S. aureus*; refer to Fig. S4B) or for 2 h (for other strains; refer to Fig. S4C) in the presence of the antibiotics. C, combined treatment. For each bacterium, both the exponential- and the stationary-phase cells were subjected to a combined treatment of antibiotic plus freezing (–196°C for 10 s), with the exponential-phase cells being frozen once and the stationary-phase cells (with the exception of *P. aeruginosa*; Fig. 4A) three times, and the cells were then subjected to the bacterial survival assay (as presented in Fig. S5). The levels of sensitivity of the exponential-phase cells and the stationary-phase cells are indicated before and after the slash (“/”), respectively, and are defined as follows: +++, highly sensitive; ++, sensitive; +, slightly sensitive; –, insensitive. Tom, tobramycin; Genta, gentamicin; Strep, streptomycin; Kana, kanamycin.

(Fig. S4C); (ii) *Bacillus subtilis* is sensitive in its exponential-phase stage but not in its stationary-phase stage; (iii) *Staphylococcus epidermidis* CMCC26069 is only slightly sensitive in its stationary-phase stage; and (iv) *Micrococcus luteus* CMCC 28001 is insensitive. The levels of sensitivity of each bacterium to antibiotic alone and to combined treatment are summarized in Table 1. These studies, though not exhaustive, suggested that, overall, Gram-negative bacteria are more sensitive to the combined treatments of aminoglycoside and freezing than Gram-positive bacteria.

Freezing facilitates killing of *P. aeruginosa* by aminoglycoside persisters in mice. *P. aeruginosa* is a multidrug-resistant pathogen associated with serious illnesses such as cystic fibrosis and traumatic burns. It was reported previously that isolates of *P. aeruginosa* from patients at a late stage of cystic fibrosis produce higher levels of antibiotic-tolerant persister cells and that such increased persister formation is their sole mechanism for surviving chemotherapy (5, 42). Here, we prepared *P. aeruginosa* persisters by the use of the same method as that used on the *E. coli* cells and found that the combined treatment of aminoglycoside and freezing was able to eradicate such *P. aeruginosa* persisters in a PMF-independent manner (Fig. S6), a scenario similar to the aforementioned observations on *E. coli* persisters (Fig. 2; see also Fig. S2).

Freezing (cryotherapy or cryosurgery) has been widely and long applied as a physical therapy to treat a number of diseases and disorders (43, 44) and even to treat skin, prostate, and lung cancers (43–46), although it damages animal cells and tissues (47, 48). Here, we demonstrated, as a proof of concept, that freezing was able to facilitate aminoglycoside eradication of *P. aeruginosa* persisters in animals based on the following observations. First, we removed muscles from sacrificed mice and then placed stationary-phase *P. aeruginosa* cells (premixed with tobramycin) on the muscles before freezing them with liquid nitrogen. Our bacterial survival assay showed that freezing significantly potentiated tobramycin against *P. aeruginosa* cells under such *in situ* conditions (column 4 versus column 3 in Fig. 5A).

Second, we employed the mouse tail as a model, considering that it is convenient to immerse the tail of a live animal in liquid nitrogen. To this end, we anesthetized mice, placed stationary-phase *P. aeruginosa* cell culture containing tobramycin on the tails, wrapped the tails with Parafilm, and immersed them in liquid nitrogen (refer to Fig. S7A). Bacterial survival assay results show that freezing at –196°C significantly ($P < 0.001$) enhanced the bactericidal effects of tobramycin on *P. aeruginosa* cells in comparison with room temperature (Fig. 5B [see also Fig. S7B]).

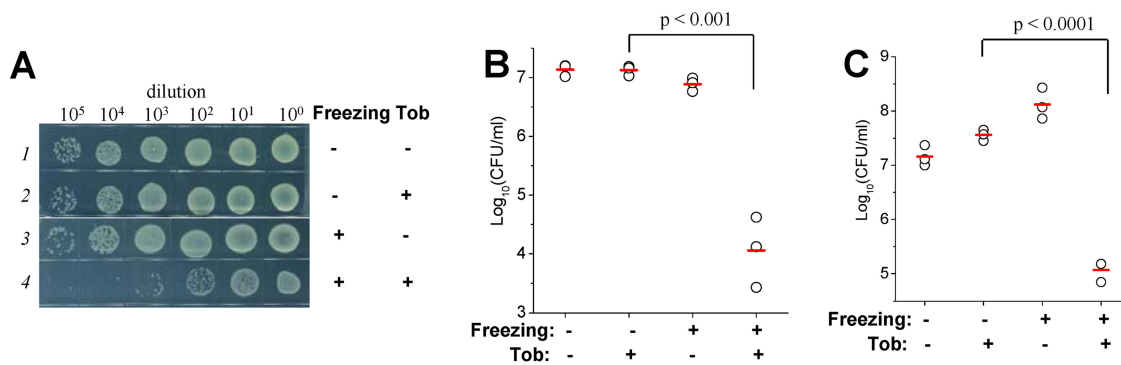


FIG 5 Freezing facilitates tobramycin killing of *P. aeruginosa* in a mouse model. (A) Survival of stationary-phase *P. aeruginosa* cells after the cells were mixed with 100 μg/ml tobramycin, plated on a piece of mouse muscle, and subjected to freezing in liquid nitrogen for 1 min. Cells were taken from the muscle and plated onto LB agar dishes. (B) Survival of stationary-phase *P. aeruginosa* cells after the cells were mixed with 100 μg/ml tobramycin, plated on the tail of an anesthetized mouse, and subjected to freezing in liquid nitrogen for 2 min. Tail lysates were plated on LB agar dishes for cell survival assay. (C) Survival of CCCP-pretreated *P. aeruginosa* cells in the wounds of mice. Cell survival assay results are presented in the middle part of Fig. S7E. Data in panels B and C are presented as means ± SD of results from three replicates.

Third, we utilized an acute skin wound model (49) to show the *in vivo* efficacy of the combined treatment. To this end, a piece of skin 1 cm by 1 cm in size was removed from the right back of anesthetized mice. *P. aeruginosa* cells were placed on the wound, tobramycin-containing culture medium was added, and the wound was subsequently subjected to a freezing treatment and bandaged (Fig. S7C). Initially, we examined stationary-phase *P. aeruginosa* cells and observed only a marginal freezing-induced tobramycin potentiation effect (Fig. S7D). Then we examined exponential-phase *P. aeruginosa* cells and observed a substantial tobramycin potentiation effect of freezing (Fig. S7E, left), particularly against both CCCP-pretreated and chloramphenicol-pretreated cells (middle and right parts). Quantification analysis revealed that freezing could significantly ($P < 0.0001$) potentiate tobramycin against CCCP-pretreated *P. aeruginosa* cells in an acute skin wound model (Fig. 5C). As expected, the frozen wounds became black overnight postsurgery (Fig. S7F), presumably due to freezing injury.

Freezing-induced aminoglycoside potentiation is suppressed by decreasing the cooling rate, by increasing the warming rate, and by the presence of cryoprotectants. We attempted to uncover the molecular mechanism underlying freezing-induced aminoglycoside potentiation. Nevertheless, these efforts were substantially compromised by our current limited understanding of the mechanism of freezing injury on cells (47, 48, 50–52). The extent of the effect of freezing injury on specific cells seems to depend on three major variables: the cooling rate, the warming rate, and the type and concentration of protective additives (48). Therefore, we examined the effects of these variables.

First, we show that the cooling rate is critical for the freezing-induced aminoglycoside potentiation. When the cooling rate of freezing was decreased by placing the bacterium-containing PCR tube in a –80°C freezer rather than immersing it in ethanol at –80°C, the bactericidal effects of tobramycin were remarkably compromised (line 5 versus line 4 in Fig. 6A). An additional decrease in the cooling rate resulted in a much lower level of cell death (lines 6 and 7 in Fig. 6A). These observations indicate that rapid freezing potentiates aminoglycoside much more effectively than slow freezing, illustrating a critical role of intracellular ice formation in bacteria in the potentiation effect according to cryobiological studies (48, 53).

Second, we found that the freezing-induced aminoglycoside potentiation was augmented if the rapidly frozen cells were thawed slowly. When the rapidly frozen *E. coli* cells were thawed in a 30°C water bath (line 6 in Fig. 6B), in an ice-water bath (line 7), or in a 4°C refrigerator (line 8), the time required for their full thawing was around 1.5, 10, or 15 min, respectively, and the cell death ratio was significantly augmented

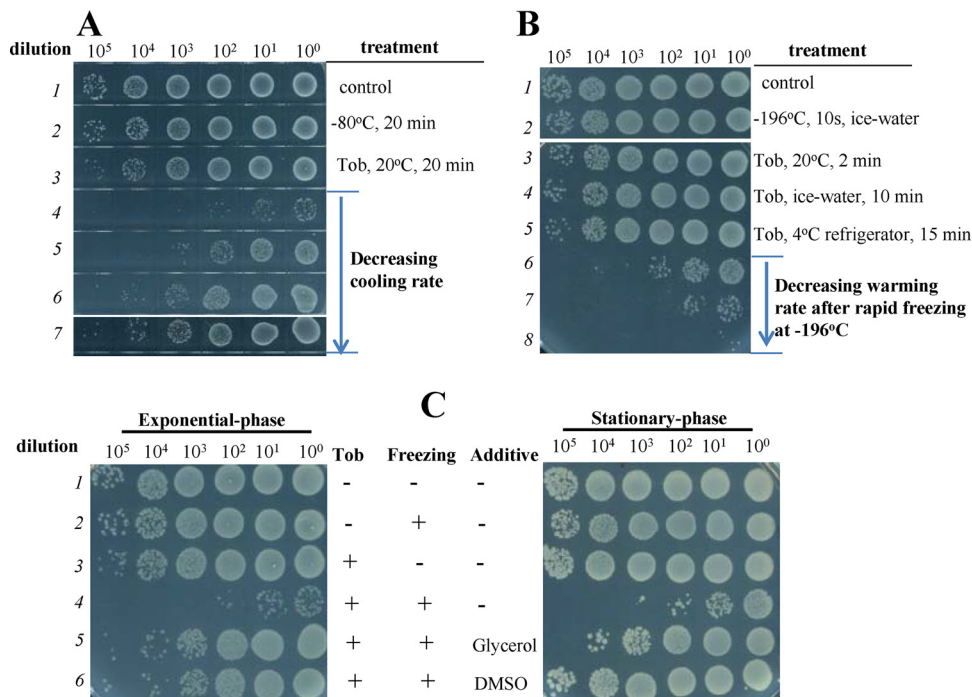


FIG 6 Effects of cooling rate, warming rate, and cryoprotectants on tobramycin potentiation. (A) Survival of exponential-phase *E. coli* cells following freezing treatment in ethanol prechilled at -80°C (line 4) or in a -80°C freezer without (line 5) or with (lines 6 and 7) an additional package of tubes (for details, see Materials and Methods), in the presence of $25\ \mu\text{g/ml}$ tobramycin. (B) Survival of exponential-phase *E. coli* cells after the cells were frozen in liquid nitrogen for 10 s in the presence of $25\ \mu\text{g/ml}$ tobramycin and then thawed at different warming rates (line 6, a 30°C water bath; line 7, an ice-water bath; line 8, a 4°C refrigerator). (C) Survival of exponential-phase (left) and stationary-phase (right) *E. coli* cells after the cells were mixed with tobramycin at concentrations of 25 and $100\ \mu\text{g/ml}$, respectively, and then subjected to freezing/thawing treatment once or three times, respectively, in the presence of 20% glycerol or 10% DMSO.

upon slower warming. This observation, in conjunction with the general views from cryobiological studies (48, 52), suggests that recrystallization of intracellular ice crystals due to slow warming plays a critical role in freezing-induced aminoglycoside potentiation.

According to cryobiological studies (50, 52), the freezing behavior of cells can be modified by cryoprotectants, which affect the rates of water transport, nucleation, and crystal growth and collectively reduce freezing injury and cell death. Here, we found that glycerol and dimethyl sulfoxide (DMSO), two cryoprotectants widely used for cell preservation (53), largely diminished the freezing-induced aminoglycoside potentiation for both exponential-phase and stationary-phase *E. coli* cells (lines 6 and 5 versus line 4 in Fig. 6C). Collectively, these observations suggest that the freezing-induced aminoglycoside potentiation is linked to the freezing injury to bacterial cells.

Freezing-induced aminoglycoside potentiation is linked to freezing injury of the cell membrane. Prompted by cryobiological studies revealing that the cell membrane (mostly in eukaryotic cells) is the primary site of freezing injury (48, 50, 53, 54), we examined whether freezing causes damage to *E. coli* cell membranes by a combination of membrane integrity staining, protein leakage assay, membrane permeability assay, and membrane morphology analysis. To this end, first, we found that the hydrophobic fluorescent probe 1-N-phenyl-naphthylamine (NPN), which fluoresces weakly in aqueous environments but becomes strongly fluorescent when interacting with the hydrophobic tail of membrane phospholipids (55), exhibited a much higher fluorescence intensity upon binding to the frozen *E. coli* cells than to untreated cells (column 2 versus column 1 and column 4 versus column 3 in Fig. 7A). This shows that the cell membrane of the frozen *E. coli* cells was damaged to a certain extent.

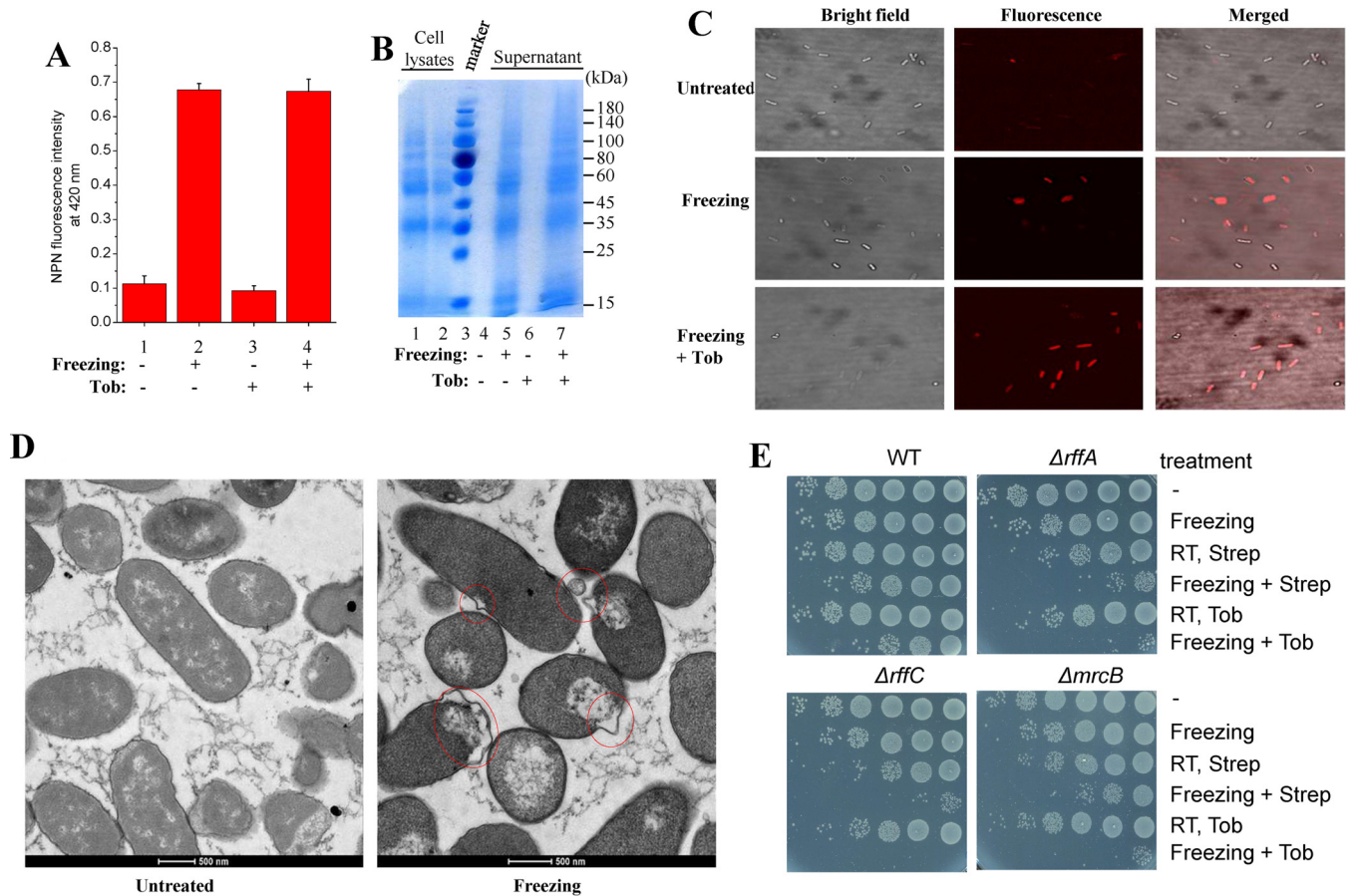


FIG 7 *E. coli* cell membranes are damaged upon freezing. (A) Fluorescence intensity of NPN after a 5-min incubation with stationary-phase *E. coli* cells. Cells were resuspended in HEPES buffer and subjected to three cycles of freezing in liquid nitrogen and thawing in ice water before mixing with 10 μ M NPN was performed. (B) SDS-PAGE analysis results from the supernatant of stationary-phase *E. coli* cells after undergoing indicated treatments. Proteins in the supernatant were concentrated 10-fold by precipitation with 10% trichloroacetic acid before electrophoresis. Lane 1, whole-cell extract; lane 2, 2-fold diluted whole-cell extracts. (C) Fluorescence microscopy imaging of exponential-phase *E. coli* cells, which were frozen, thawed, and incubated with 50 μ g/ml PI for 10 min before imaging. (D) Transmission electron micrographs of exponential-phase *E. coli* cells following freezing treatment. (E) Survival of exponential-phase *E. coli* cells of the indicated genotypes following 10-s treatment with tobramycin or streptomycin plus freezing in liquid nitrogen. Results for other mutant strains are presented in Fig. S8C. RT, room temperature; WT, wild type.

Second, we examined the effects of freezing on the leakage of intracellular proteins. Results of SDS-PAGE analysis of proteins present in the cell suspension medium indicate that freezing treatment enables a significant portion (around 10%) of cellular proteins to leak out (lanes 5 and 7 in Fig. 7B), in line with earlier reports showing that intracellular content of bacterial, mammalian, and plant cells had leaked out after freezing (56–59). In contrast, unfrozen cells, in either the absence or presence of tobramycin, did not show any detectable cellular proteins in the medium (lanes 4 and 6 in Fig. 7B).

Third, we evaluated the cell membrane permeability of *E. coli* cells upon freezing by using propidium iodide (PI), a fluorescent probe widely used for DNA staining in membrane-permeabilized cells (60) (particularly dead cells). We found that many more *E. coli* cells were stained by PI after freezing than in the absence of freezing treatment, as revealed by fluorescence microscopic analysis (Fig. 7C) and flow cytometry analysis (Fig. S8A). Last but not least, thin-section transmission electron microscopic analysis revealed that the untreated *E. coli* cells exhibited regular cell morphology, while the frozen cells showed abnormalities in their cell envelopes, including the appearance of vesicles, bulges, and wrinkles (as highlighted by red circles in Fig. 7D).

Furthermore, we provide genetic evidence to show that aminoglycoside potentiation is linked to freezing injury on the cell membrane of bacteria. Initially, the Keio collection (a widely used *E. coli* genome-wide single-gene deletion library [61]) was

subjected to freezing sensitivity screening test in our laboratory (data to be published elsewhere). Forty-one mutants were identified as hypersensitive, with deletion of genes related to ribosome biogenesis, tRNA modification, cell division, and membrane biogenesis and stability (Fig. S8B). Of these 41 mutants, some mutants potentially have a destabilized cell membrane due to a defect in lipopolysaccharide biosynthesis ($\Delta rffA$, $\Delta rffC$, $\Delta rffD$, and Δrfe mutants), peptidoglycan biosynthesis ($\Delta mrcB$ mutant), or membrane protein biogenesis ($\Delta degP$ mutant); these were selected for further examination. The $\Delta rffA$, $\Delta rffC$, and $\Delta mrcB$ mutants were much more sensitive to the combined treatment of aminoglycoside (streptomycin and/or tobramycin) and freezing than the BW25113 wild-type strain (Fig. 7E), and the $\Delta rffD$, Δrfe , and $\Delta degP$ mutants were also more sensitive (Fig. S8C). Collectively, these observations demonstrate that the cell membrane of *E. coli* cells is substantially damaged upon freezing and thawing, which may directly or indirectly contribute to the freezing-enhanced aminoglycoside uptake and thus to potentiation.

The mechanosensitive ion channel MscL directly mediates the freezing-enhanced bacterial uptake of aminoglycoside. Previously, Blount and coworkers uncovered a direct role of the mechanosensitive ion channel MscL in transportation of the aminoglycoside dihydrostreptomycin under conventional treatment conditions (62, 63). We thus systematically examined *E. coli* mutants lacking the *mscL* gene or other *mscL*-related, *mscS*-like mechanosensitive ion channel genes (i.e., *mscS*, *mscK*, *mscM*, *ynal*, *ybdG*, and *ybiO*) (64). Nevertheless, none of these single-gene deletion mutants exhibited increased resistance to the combined treatment of aminoglycoside and freezing at the stationary-growth state (Fig. S8D).

We did observe, however, a marginal increase in the resistance to the combined treatment for $\Delta mscL$ exponential-phase cells (Fig. S8E). Prompted by this observation, we analyzed the effects of MscL on *E. coli* MJF612, which lacks the genes of four ion channels (i.e., *mscL*, *mscS*, *mscK*, and *ybdG*) (62, 65). Data presented in Fig. 8A indicate that complementary expression of MscL, but not of MscS, MscK, or YbdG, dramatically increased the sensitivity of MJF612 to the combined treatment consisting of addition of streptomycin and freezing (only streptomycin was analyzed due to the cross-resistance of MJF612 to tobramycin and gentamicin as a result of the presence of its kanamycin resistance gene; Fig. S8F). Consistently, we found that streptomycin, as extracted from frozen MJF612 cells complementarily expressing MscL but not MscS, suppressed bacterial cell growth (red frame in Fig. 8B), thus indicating a direct role of MscL in transporting streptomycin during freezing treatment.

To further demonstrate that MscL directly mediates aminoglycoside uptake of *E. coli* cells upon freezing and also identify the physiological conditions under which MscL significantly contributes to the freezing-induced aminoglycoside potentiation, we screened *E. coli* wild-type cells (BW25113 strain) in different states and examined whether their sensitivity to the combined treatment of tobramycin and freezing was correlated with the protein levels of endogenously expressed MscL. First, we found that *E. coli* exponential-phase cells, which were cultured either in normal LB medium or in NaCl-free LB medium, were much more sensitive to the combined treatment than stationary-phase cells (Fig. S9A). Meanwhile, the MscL protein levels in the exponential-phase cells were higher than in stationary-phase cells (lane 1 versus lane 2 and lane 3 versus lane 4 in Fig. 8C).

Second, when stationary-phase *E. coli* cells cultured in Mueller-Hinton broth (MHB) medium were transferred to M9 medium for preparation of starvation-induced persisters (41), they became much more tolerant to the combined treatment (Fig. 8D), and the MscL protein levels concomitantly decreased (lane 9 versus lane 10 in Fig. 8C). Third, *E. coli* exponential-phase cells cultured in M9 medium plus glucose became much more sensitive to the combined treatment after sucrose-mediated hyperosmotic shock (Fig. S9B), and the MscL protein levels concomitantly increased (lane 6 versus lane 5 in Fig. 8C). The same was observed for nutrient shift-induced *E. coli* persisters (Fig. S9C; lane 7 versus lane 8 in Fig. 8C), which were prepared by transferring *E. coli* exponential-phase cells from M9 medium plus glucose to M9 medium plus fumarate medium (41).

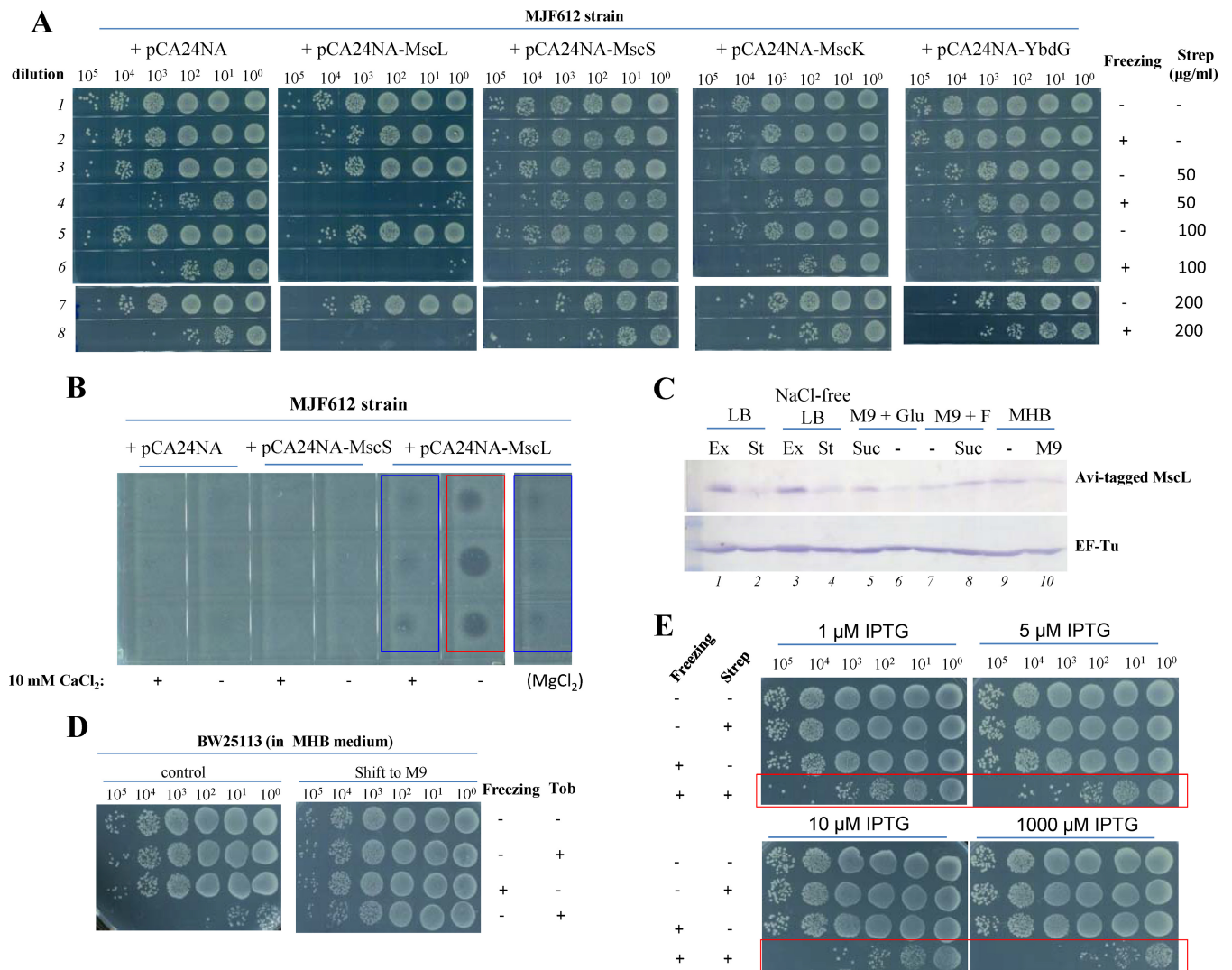


FIG 8 The MscL channel mediates the uptake of streptomycin by *E. coli* cells upon freezing. (A) Survival of exponential-phase *E. coli* cells of the indicated genotypes. *E. coli* MJF612 cells (Frag1 $\Delta mscL::cm$, $\Delta mscS$, $\Delta mscK::kan$, $\Delta ybdG::aprD$) were transformed with the indicated plasmids for expressing each channel and then subjected to the combined treatment consisting of addition of streptomycin and freezing before cell survival assay. (B) Growth inhibition of *E. coli* cells on LB agar dishes by streptomycin as extracted from *E. coli* cells of the indicated genotypes that had been treated as indicated. (C) Immunoblotting analysis results showing the protein levels of endogenously expressed MscL in *E. coli* cells under the indicated culturing conditions. EF-Tu was analyzed as a sample-loading control. Ex, exponential-phase growth; St, stationary-phase growth; Suc, osmotic shock with 1.25 M sucrose; Glu, 5 g/liter glucose; F, 2 g/liter fumarate; “-”, untreated. (D) Survival of stationary-phase *E. coli* BW25113 cells, which were cultured in MHB medium, transferred to M9 medium, and cultured for 5 h before being subjected to the combined treatment of tobramycin and freezing. (E) Survival of MscL-expressing *E. coli* MJF612 cells following the combined treatment consisting of addition of streptomycin and freezing. MscL expression was induced to different degrees (Fig. S9D) by the indicated concentrations of IPTG.

Last, we artificially induced MscL protein expression in *E. coli* MJF612 cells with increasing concentrations (1 µM, 5 µM, 10 µM, and 1,000 µM) of IPTG (isopropyl β-D-1-thiogalactopyranoside). With increasing IPTG concentrations, the MscL protein levels increased (lanes 1 to 4 in Fig. S9D), and the cells were increasingly sensitive to the combined treatment consisting of addition of streptomycin and freezing (red frame in Fig. 8E). These data, together with the results reported previously by Blount and coworkers showing a role of MscL in transporting streptomycin under conventional treatment conditions (62, 63), strongly suggest that MscL directly mediates the uptake and potentiation of aminoglycosides during freezing treatment.

MscL-mediated aminoglycoside uptake upon freezing is inhibited by Ca²⁺/Mg²⁺. In the streptomycin uptake assay, we observed that the presence of 10 mM Ca²⁺ or Mg²⁺ significantly reduced the MscL-mediated uptake of streptomycin in *E. coli*

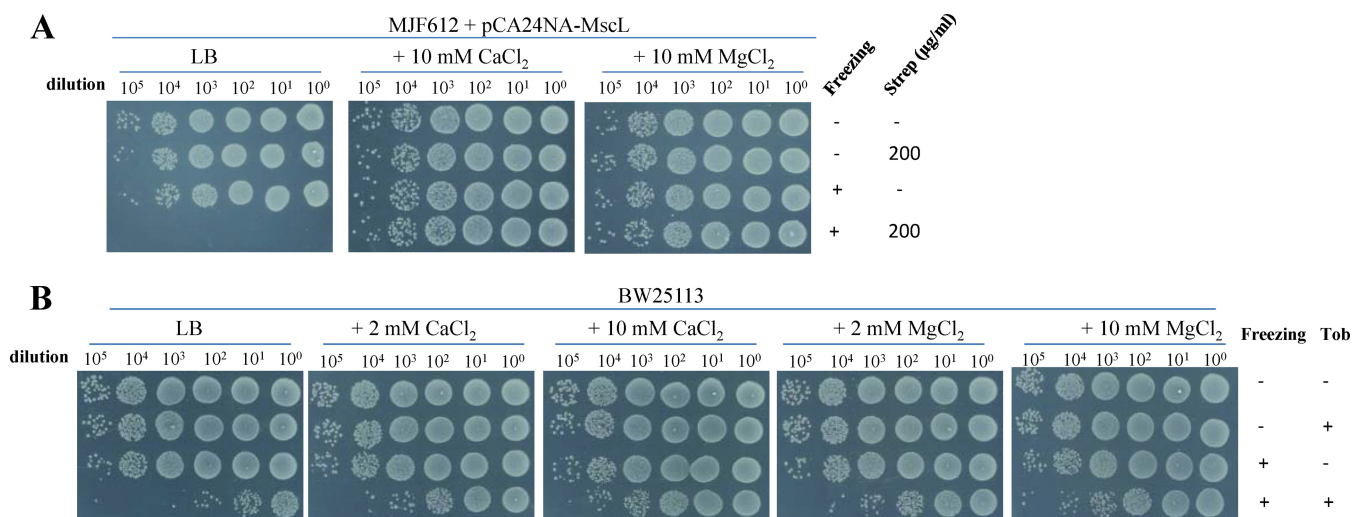


FIG 9 MscL-mediated uptake of streptomycin upon freezing is suppressed by Ca²⁺/Mg²⁺. (A and B) Survival of exponential-phase *E. coli* MJF612 cells complementarily expressing MscL (A) and BW25113 cells (B) following a 10-s treatment consisting of addition of streptomycin and freezing in the absence or presence of CaCl₂ or MgCl₂.

MJF612 cells (blue frames versus red frame in Fig. 8B). In line with these observations, the presence of 10 mM Ca²⁺ or Mg²⁺ also abolished the freezing-induced streptomycin potentiation in MJF612 cells complementarily expressing MscL (Fig. 9A). These observations thus provide additional evidence that MscL mediates aminoglycoside uptake under freezing conditions. To evaluate the effects of Ca²⁺ and Mg²⁺ in the context of a wild-type genetic background, we analyzed *E. coli* BW25113 cells. Our results (Fig. 9B) indicate that both Ca²⁺ and Mg²⁺ were able to significantly suppress the freezing-induced aminoglycoside potentiation (Fig. 9A), while K⁺ and Na⁺ had no significant effects (Fig. S9E).

DISCUSSION

The major findings in our study include (i) the potentiation effect of rapid freezing on aminoglycoside action against both normal bacterial cells and antibiotic-tolerant persisters (Fig. 1, 2, and 4; see also Fig. S6 in the supplemental material) (Table 1) and (ii) a direct role of the mechanosensitive ion channel MscL in mediating such potentiation (Fig. 8 and 9; see also Fig. S9). Not surprisingly, the potentiation effect is achieved by enhancing the bacterial uptake of aminoglycosides. Remarkably, this freezing-enhanced uptake is PMF and ATP independent (Fig. 2C and 3C; see also Fig. S2 and S6). These results contrast with the metabolite-stimulated PMF-dependent potentiation of aminoglycosides (18–22) and the PMF-dependent bacterial uptake of aminoglycosides under conventional conditions (as extensively reviewed in reference 38).

Cell membrane destabilization-induced MscL activation contributes to freezing-enhanced aminoglycoside uptake. Although aminoglycoside antibiotics have been used clinically since the antituberculosis drug streptomycin was discovered in the 1940s, their mechanisms of action remain enigmatic (18, 66–68), including how they are taken up by bacterial cells (38). It is generally accepted that the bacterial uptake of aminoglycosides is initiated by their ionic binding to the surface of bacterial cells, followed by two energy-dependent phases, i.e., EPDI and EPDII, which represent a low rate of energized uptake and a rapid energy-dependent accumulation of aminoglycosides that also requires protein synthesis, respectively (38). Nevertheless, the nature of transporters or carriers responsible for such energy-dependent translocation of the positively charged aminoglycosides across the cytoplasmic membrane remains largely undefined (37, 38), and elucidation of the form of the energy driving the bacterial uptake of aminoglycosides also remains elusive. Although the PMF has been known to be a requisite for the uptake (reference 38 and references therein), the issue

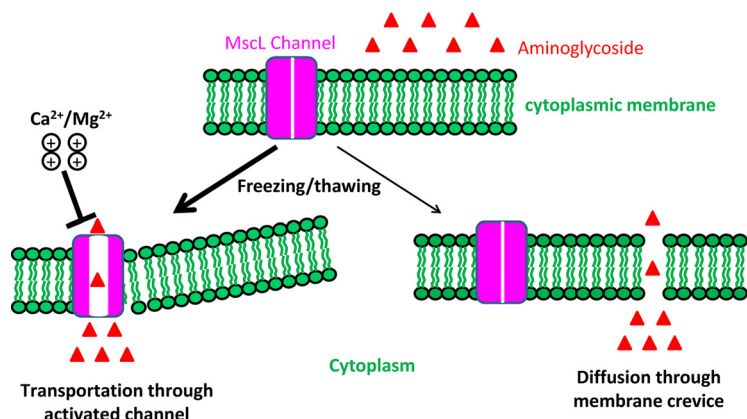


FIG 10 Freezing-induced membrane destabilization can activate the MscL channel, which in turn enhances aminoglycoside uptake. The key to the potentiation of aminoglycosides by freezing is to facilitate traversal of the cytoplasmic membrane of bacterial cells by positively charged aminoglycosides. Two conceivable mechanisms are diagrammed here. The first mechanism is transportation of aminoglycosides via ion channels (e.g., MscL), which could be caused by membrane destabilization as induced by the freezing/thawing treatments, and divalent cations such as Ca^{2+}/Mg^{2+} can also be transported by the activated MscL and thus competitively inhibit aminoglycoside transportation. The second mechanism is diffusion of aminoglycosides through the crevices that are transiently formed in the destabilized cytoplasmic membrane. In light of our experimental data and observations from the literature, the MscL channel activation-based mechanism is the more likely of the two.

of whether ATP and electron transfer play a role in driving aminoglycoside uptake has not been fully resolved (69).

Our combined treatments with aminoglycoside and freezing differ from earlier reports in the following aspects. (i) The aminoglycoside exposure time in our treatment was shortened to a few minutes, rather than the couple of hours required for metabolite-induced aminoglycoside potentiation (18–21) or in other more routine methods (32, 34). (ii) The bactericidal effect and bacterial uptake of aminoglycosides in our study were unaffected by the presence of CCCP or FCCP, i.e., these effects were PMF independent. (iii) Unlike EPDII, which requires protein synthesis (as reviewed in reference 38), the enhanced aminoglycoside uptake in our protocol does not require protein synthesis (Fig. 2C; see also Fig. S2F and S6E). These revelations strongly suggest that our combined treatment approach represents a totally different scenario.

The molecular mechanisms underlying this aminoglycoside uptake are apparently linked to intracellular ice formation-induced cellular injury occurring during freezing and also during thawing, in view of the general concepts in cryobiology (48, 52, 53, 70, 71) and our observations that freezing-induced aminoglycoside potentiation was suppressed by decreasing the cooling rate (Fig. 6A), increasing the warming rate (Fig. 6B), or adding cryoprotectants (Fig. 6C). On the other hand, cell membranes (including the cytoplasmic membrane and organelle membranes in eukaryotic cells) are generally thought to be the primary site of freezing injury according to cryobiological studies (48, 50, 53, 54, 71). In line with this notion, our combined analyses by NPN staining, PI staining, protein leakage assay, and electron microscopy collectively and unambiguously revealed the injurious effects of freezing on the membranes of *E. coli* cells (Fig. 7). In particular, some membrane-destabilized *E. coli* mutants are more sensitive to freezing-induced aminoglycoside killing (Fig. 7E; see also Fig. S8C). In light of all these revelations, we suggest that freezing-enhanced aminoglycoside uptake represents a direct or indirect effect of freezing injury on the cell membrane of bacteria.

Furthermore, we propose that the freezing-enhanced aminoglycoside uptake is most likely accomplished by cytoplasmic membrane-localized ion channels such as MscL (as diagrammed in the left part of Fig. 10), based on several independent observations. First, *E. coli* $\Delta mscL$ cells exhibited a marginal increase in their resistance to the combined treatment (Fig. S8E). Second, only the complementary expression of the MscL channel, but not that of MscS, MscK, and YbdG channels, dramatically

increased the sensitivity of MJF612 cells to the combined treatment (Fig. 8A). Third, the complementary expression of MscL, but not MscS, enabled MJF612 cells to take up much more streptomycin (Fig. 8B). Fourth, we found five physiological conditions under which the endogenously expressed MscL in *E. coli* cells was upregulated (Fig. 8C) and the sensitivity of the cells to the combined treatment of tobramycin and freezing was increased concomitantly (Fig. 8D; see also Fig. S9A to C). Last but not least, we observed a strong association between the sensitivity of the MJF612 cells to the combined treatment and the protein levels of the complementarily expressed MscL (Fig. 8E; see also Fig. S9D). Additional evidence supporting that interpretation of this MscL activation-based mechanism includes the following. First, the pore size of MscL is around 30 Å (72), which is large enough to allow aminoglycosides to flow in. Second, MscL activation does not require PMF and ATP, consistent with our observations. Collectively, our observations, in conjunction with studies from Blount and coworkers on the MscL-mediated uptake of dihydrostreptomycin under conventional treatment conditions (62, 63), strongly suggest that MscL directly mediates aminoglycoside uptake under freezing conditions.

MscL, a mechanosensitive ion channel, is well known to be activated in response to changes in membrane tension as elicited by osmotic shock, cold/heat shock stresses, and/or other types of mechanical forces (73–75). Conceivably, freezing leads to membrane damage and destabilization (Fig. 7) (48, 50, 53, 54), which, in turn, changes the membrane tension and thus activates MscL. Alternatively, freezing can directly result in osmotic shock (48, 52, 71), which, in turn, could also activate MscL (73, 74). It should be pointed out that besides MscL, other unidentified proteins, likely homologs of MscL, appear to also mediate the freezing-induced aminoglycoside potentiation in *E. coli*, given that the *E. coli* $\Delta mscL$ stationary-phase cells exhibited sensitivity comparable with that of the wild-type cells (Fig. S8D) and that the exponential-phase $\Delta mscL$ cells were still sensitive to the combined treatment (Fig. S8E).

Notably, the presence of $\text{Ca}^{2+}/\text{Mg}^{2+}$ significantly suppressed the MscL-enhanced aminoglycoside uptake (Fig. 8B) and potentiation (Fig. 9A) upon freezing. One may suspect that such suppression results from the effects of Ca^{2+} or Mg^{2+} on *E. coli* cells for protection from freezing-induced injury. Our cell survival assay revealed that neither Ca^{2+} nor Mg^{2+} protected *E. coli* cells from being killed by three cycles of freezing treatments (Fig. S9F). In addition, our SDS-PAGE analysis results show that neither Ca^{2+} nor Mg^{2+} suppressed the freezing-induced leakage of cellular proteins (Fig. S9G). Therefore, the suppressive effects of Ca^{2+} and Mg^{2+} more likely result from their direct actions on MscL. Given that Ca^{2+} can be transported from bacterial cells by the MscL channel (64, 76) and that MscL is able to nonspecifically transport ions to a certain degree (77), it is conceivable that Ca^{2+} and Mg^{2+} can also be transported into cells by freezing-activated MscL. As such, high (up to 10 mM) concentrations of Ca^{2+} and Mg^{2+} in cell suspensions would be able to competitively inhibit MscL-mediated aminoglycoside uptake (as diagrammed in Fig. 10) at a concentration of aminoglycoside of around 100 μM .

Another possible explanation for the freezing-induced aminoglycoside potentiation is that crevices or pores are formed in the cytoplasmic membrane of bacterial cells during the freezing/thawing treatment, such that aminoglycosides are able to freely diffuse through these crevices (as illustrated in the bottom right part of Fig. 10). This hypothesis is supported by the observations that freezing leads to (i) leakage of a large amount of cellular proteins (Fig. 7B) and other intracellular content (56–59) from the cells, (ii) increased permeability of the cell membrane (Fig. 7C; see also Fig. S8A), and (iii) cell membrane bending and wrinkles (Fig. 7D). Accordingly, this mechanism is PMF and ATP independent. Nevertheless, this mechanism cannot well explain why different types of aminoglycoside antibiotics with similar chemical structures and molecular weights differ in their bactericidal effects against one bacterium upon freezing (Table 1), assuming that their free diffusion rates through the membrane crevice would be basically equal. It also cannot explain why the presence of divalent cations (e.g., Ca^{2+} and Mg^{2+}) can suppress the freezing-induced aminoglycoside

uptake and potentiation. These contradictions, however, can be well explained by the MscL channel activation-based mechanism, which thus represents a more favorable hypothesis.

Potential applications for freezing-induced aminoglycoside potentiation in eradicating multidrug-tolerant persisters. Biological effects and the underlying mechanisms of freezing have long been investigated as an important aspect of cryobiology, which is a multidisciplinary science for the study of the physical and biological behaviors of cells and tissues at low temperatures (47, 48, 50, 51, 53). Advances in this field have facilitated the development of procedures for the preservation of cells of biological, medical, and agricultural significance (51) and for treating a number of diseases (e.g., skin conditions such as warts, moles, skin tags, and solar keratoses) (43, 44). Importantly, freezing has been utilized to treat skin, prostate, lung, and other types of cancers (43–46) (termed cryotherapy or cryosurgery). To the best of our knowledge, our study is the first report of its application in treating bacterial infections, possibly because the bactericidal effects of freezing alone on bacterial pathogens are weak (Fig. 1 and 4; see also Fig. S5) (71). A direct application of our combined treatment protocol to the eradication of persister bacterial cells would obviously be limited due to the inevitable freezing injury to animal cells and tissues. Nonetheless, our work is still of interest for developing promising antipersister strategies, based on the following considerations.

First, optimization of the cooling rate and the warming rate and the addition of appropriate cryoprotectants may minimize the freezing injury on the infected site of the animals or humans (48, 53) but meanwhile maintain the efficiency of the combined treatment in killing pathogen persisters, as implied by the results presented in Fig. 6. In particular, those cryoprotectants that can specifically protect animal cells from freezing injury but have no beneficial effect on pathogens would be ideal for this purpose. Second, if the precise biochemical mechanisms underlying the freezing-induced activation of MscL are unraveled, new strategies, other than freezing, for example, MscL activation with small-molecule agonists, might be developed for killing bacterial persisters. Notably, Blount and coworkers recently reported that MscL agonists are able to potentiate antibiotics against pathogens under conventional conditions (78), although their potentiation effects are weaker than those of freezing as reported here.

MATERIALS AND METHODS

Strains, culture conditions, and reagents. Various Gram-negative (*E. coli*, *P. aeruginosa*, *A. baumannii*, *K. pneumoniae*, *S. flexneri*, and *S. enterica* serovar Typhimurium) and Gram-positive (*S. aureus*, *B. subtilis*, *M. luteus*, *L. lactis*, *S. epidermidis*, and *E. faecalis*) bacterial strains, *E. coli* strain MJF612 (Frag1 Δ mscL::cm, Δ mscS, Δ mscK::kan, and Δ ybdG::aprD) and mechanosensitive ion channel mutants of *E. coli* (i.e., Δ mscL, Δ mscS, Δ mscK, Δ mscM, Δ ynal, Δ ybdG, and Δ ybiO mutants) were used in this study, and their characteristics are described in Table S1A in the supplemental material. Briefly, an overnight culture of each strain was diluted at 1:500 in Luria-Bertani (LB) medium (note that the MRS medium was used for *L. lactis* and *E. faecalis*) and agitated in a shaker (37°C, 220 rpm) for 3 to 6 h and 20 to 24 h to prepare exponential-phase and stationary-phase cells, respectively. The antibiotics used in our study included tobramycin, streptomycin, gentamicin, kanamycin, ampicillin, carbenicillin, ofloxacin, ciprofloxacin, chloramphenicol, rifampin, and erythromycin, and their manufacturers and final concentrations for different treatments are described in Table S1B. Carbonyl cyanide m-chlorophenyl hydrazone (CCCP) was purchased from Sigma-Aldrich and 3 H-labeled tobramycin from American Radiolabeled Chemicals, Inc. (catalog no. ART1927, lot no. 160429). All other chemical reagents were of analytical purity.

Treatment of bacteria with aminoglycosides and rapid freezing. Exponential-phase (optical density at 600 nm [OD₆₀₀] = 0.8) or stationary-phase cultures of *E. coli*, *P. aeruginosa*, and *S. aureus* cells were transferred to Eppendorf tubes (100 μ l) and mixed thoroughly with each antibiotic at the final concentrations described in Table S1B and then immediately immersed in liquid nitrogen (–196°C) for 10 s or in prechilled ethanol (–80°C) for 20 s and subsequently thawed in an ice-water bath (with the procedure usually being completed within 10 min). For stationary-phase cells, one, two, or three rounds of freezing and thawing treatments were performed. Treated cells were washed twice using phosphate-buffered saline (PBS; 0.27 g/liter KH₂PO₄, 1.42 g/liter Na₂HPO₄, 8 g/liter NaCl, 0.2 g/liter KCl, pH 7.4) by centrifugation (13,000 \times g, 30 s), and then 5 μ l of 10-fold serially diluted cell suspension was spot plated onto LB agar dishes for survival assay. Other types of bacterial strains were treated similarly.

Effects of freezing time, cooling rate, warming rate, and cryoprotectants on aminoglycoside potentiation. To prolong the duration of the frozen state, the bacterium-containing Eppendorf tubes

were immersed in liquid nitrogen or prechilled ethanol for various lengths of time (10 and 20 s and 1 and 3 min). Slow cooling was achieved by packaging the bacterium-containing PCR tube with an Eppendorf tube, which was additionally packed with a 15-ml plastic tube and then placed in a -80°C refrigerator for 20 min. Slow warming and rapid warming of the rapidly frozen cells at -196°C were achieved by thawing them in a 4°C refrigerator and in a 30°C water bath, respectively, and the bacterial cells were then immediately washed after full thawing that was usually completed within 15 and 1.5 min, respectively. The effects of the cryoprotectants were examined by mixing the cell cultures with glycerol and DMSO at final concentrations of 20% and 10%, respectively, before freezing.

Preparation and eradication of persister and persister-like cells. Persister cells were prepared by adding ampicillin ($100\ \mu\text{g}/\text{ml}$) or ofloxacin ($5\ \mu\text{g}/\text{ml}$) into the exponential-phase *E. coli* cells (OD_{600} of approximately 0.8) followed by continuous agitation for another 3 h according to a method described in earlier reports (32–34). Ofloxacin-tolerant *P. aeruginosa* persisters were prepared similarly by treating cells with ofloxacin ($2.5\ \mu\text{g}/\text{ml}$). The cells were then concentrated 10-fold or 100-fold via centrifugation and resuspension, and they were subsequently thoroughly mixed with each type of aminoglycoside antibiotic at the concentrations indicated in Table S1B before being subjected to the rapid freezing treatment and survival assay as described above. For preparing persister-like cells, exponential-phase cultures of *E. coli* or *P. aeruginosa* cells were agitated with CCCP ($20\ \mu\text{M}$), chloramphenicol ($35\ \mu\text{g}/\text{ml}$), erythromycin ($20\ \mu\text{g}/\text{ml}$), rifampin ($100\ \mu\text{g}/\text{ml}$), or sodium azide ($6\ \text{mM}$) at 37°C for 1 h and then mixed thoroughly with tobramycin ($25\ \mu\text{g}/\text{ml}$). These cells were subjected to the rapid freezing treatment and survival assay with or without having been subjected to further agitation at 37°C for 1 h.

Aminoglycoside pretreatment followed by rapid freezing. Each type of aminoglycoside antibiotic was added to stationary-phase *E. coli* cell cultures at the concentrations indicated in Table S1B, and the cultures were continuously agitated at 37°C for 3 additional hours. The cell cultures were then transferred into Eppendorf tubes, and 1, 2, or 3 cycles of rapid freezing (in liquid nitrogen) and thawing (in ice water) were performed before bacterial survival assay as described above. Exponential-phase *P. aeruginosa* cell cultures were supplemented with tobramycin ($12.5\ \mu\text{g}/\text{ml}$), continuously agitated at 37°C for 1, 2, or 3 h, transferred into Eppendorf tubes, and subjected to the rapid freezing treatment and survival assay.

Aminoglycoside uptake assay. The bacterial uptake of tobramycin was measured by two independent methods. In the radioactivity assay, a stock solution of $15\ \mu\text{Ci}$ ^3H -labeled tobramycin/ml was prepared in pure water and stored at -20°C . Referring to the method described in our earlier report for assaying ^3H -labeled estrogen uptake in *E. coli* cells (79), exponential-phase *E. coli* cell cultures were concentrated 4-fold by centrifugation and resuspension, thoroughly mixed with ^3H -labeled tobramycin at a final concentration of $0.015\ \mu\text{Ci}$ per $100\ \mu\text{l}$, and then subjected to the rapid freezing treatment. After thawing in an ice-water bath, the cells were centrifuged ($16,000\ \text{rpm}$, 15 s), washed once with the PBS buffer, resuspended in a lysis buffer ($0.2\ \text{M NaOH}$, 1% SDS), and incubated at 90°C for 30 min. The cell lysates were then cooled, centrifuged quickly ($800\ \text{rpm}$, 10 s), and mixed with a 5-volume scintillation cocktail before subjected to radioactivity measurement on a PerkinElmer Tri-Carb3110TR liquid scintillation analyzer. The nonradioactivity assay was performed as recently described by us (41), such that tobramycin as taken up by *E. coli* cells was extracted by cell lysis and then dropped on LB agar dishes to inhibit bacterial cell growth.

Membrane integrity analyses. (i) NPN staining. The integrity of the outer membrane of *E. coli* cells after the freezing treatment was analyzed as we previously reported (80) by recording the fluorescence intensity of NPN (1-N-phenyl-1-naphthylamine), which increases upon interacting with the hydrophobic tail of membrane phospholipids (55). Briefly, exponential-phase *E. coli* cells were resuspended in 5 mM HEPES buffer (pH 7.2), with or without the addition of $25\ \mu\text{g}/\text{ml}$ tobramycin, and then subjected to freezing in liquid nitrogen and thawing in an ice-water bath before being mixed with acetone-dissolved NPN (to reach a final concentration of $10\ \mu\text{M}$). The fluorescence intensity was recorded with a Hitachi F-4600 fluorescence spectrophotometer at the excitation and emission wavelengths of 350 and 420 nm, respectively.

(ii) Protein leakage. The integrity of the cell membrane after the freezing treatment was evaluated by examining the cellular protein leakage into the medium. For this, stationary-phase *E. coli* cells were resuspended in the PBS buffer, mixed with tobramycin ($100\ \mu\text{g}/\text{ml}$), and then subjected to the freezing treatment in liquid nitrogen and thawing in an ice-water bath three times before centrifugation at $10,000 \times g$ for 2 min. Proteins that leaked into the surrounding medium were concentrated by precipitation with 10% trichloroacetic acid, washed with acetone, and then analyzed using 10% SDS-PAGE (visualized by Coomassie blue staining).

(iii) Propidium iodide (PI) staining. Exponential-phase *E. coli* cells ($100\ \mu\text{l}$) were frozen in the absence or presence of $25\ \mu\text{g}/\text{ml}$ tobramycin and then washed and incubated at room temperature in PBS–propidium iodide (PI) ($50\ \mu\text{g}/\text{ml}$) for 10 min. Samples were analyzed on a BD Accuri C6 flow cytometer with the following settings: detector, FL2; flow rate, $14\ \mu\text{l}/\text{min}$; core size, $10\ \mu\text{m}$. Meanwhile, the treated cells were plotted on agarose after PI staining. Images were recorded at 30°C with an N-SIM imaging system (Nikon) equipped with a $100\times/1.49$ -numerical-aperture (NA) oil-immersion objective (Nikon) and laser beams ($561\ \text{nm}$).

(iv) Electron microscopy analysis. Exponential-phase *E. coli* cells ($100\ \mu\text{l}$) were frozen in the absence or presence of $25\ \mu\text{g}/\text{ml}$ tobramycin, treated with sucrose (with a final concentration of 20%) for 1 min, fixed with glutaraldehyde and formaldehyde (at final concentrations of 0.1% and 2%, respectively) for 1 h, and subjected to postfixation and dehydration. Cells were subjected to ultrathin sectioning (using a PowerTome-XL ultramicrotome) and negatively stained with 2% uranyl acetate before being imaged on a JEM-1400 transmission electron microscope operated at $80\ \text{kV}$ at a magnification of 3,000 or 25,000.

Assay of intracellular ATP levels in *E. coli* exponential-phase cells. A luciferase-based kit (catalog no. 50026B; Beyotime Biotechnology, Shanghai, China) was used to measure ATP levels according to the manufacturer's instructions. Briefly, *E. coli* exponential-phase cells, with or without pretreatment of 20 μ M CCCP or 6 mM Na₂S₂O₈ at 37°C for half an hour, were lysed using the lysis buffer and then centrifuged (12,000 \times *g*, 4°C, 5 min). The supernatant was quickly mixed with the working solution at equal volumes and then transferred into a 96-well plate before light recording on a FLUOstar Omega microplate reader was performed using the Luminometer method. Cells treated with rapid freezing for 10 s with liquid nitrogen were also analyzed.

Proton motive force assay. A flow cytometry-based assay was applied to measure the proton motive force by using the fluorescence probe 3,3'-diethyloxycarbocyanine iodide [DiOC2(3)] (purchased from MaoKang Biotechnology, Inc., Shanghai, China) according to the manufacturer's instructions. Briefly, *E. coli* exponential-phase cells, with or without CCCP pretreatment for 1 h, were diluted into PBS to a cell density of 10⁶ cells/ml and incubated with DiOC2(3) (at a final concentration of 30 μ M) at room temperature for 15 min. Cells were subjected to flow cytometric analysis on a FACSymphony A5 system (BD Biosciences) with excitation at 488 nm and emission in both the red (630-nm) channel and green (515-nm) channel. Cells treated by rapid freezing for 10 s with liquid nitrogen were also analyzed.

Animal experiments. Eight-week-old ICR male mice (around 28 g in body weight) were purchased from the Animal Center of Fujian Medical University and maintained in the Animal Center of Fujian Normal University. Mice were housed for 1 or 2 days and then randomly divided into four groups for surgery experiments (group A, room temperature without tobramycin; group B, room temperature with tobramycin; group C, freezing without tobramycin; group D, freezing with tobramycin; *n* = 3). Briefly, after anesthetization by intraperitoneal injection of 4% chloral hydrate, the tails of the mice were sterilized using 70% ethanol, and 30- μ l stationary-phase cultures of *P. aeruginosa* cells premixed with 100 μ g/ml tobramycin were seeded on the tails. After full absorption and drying, the mice tails were wrapped with Parafilm and then immersed in liquid nitrogen for 2 min. The mice were sacrificed half an hour later, and the tails were cut and homogenized in 2 ml PBS buffer, with the lysates being spot plated on LB agar dishes for bacterial survival assay.

The muscle of the sacrificed mice from group A was cut and placed in Eppendorf tubes for conducting the *in situ* freezing studies. Briefly, 5 μ l tobramycin-containing stationary-phase cultures of the *P. aeruginosa* cells were spot plated on these tissues and then subjected to freezing treatment in liquid nitrogen for 1 min. After addition of 2 ml PBS buffer, the mixtures were shaken for 5 min and the remaining supernatant was spot plated on LB agar dishes for bacterial survival assay.

In addition, we applied a skin acute wound model to evaluate the efficacy of the combined treatment. Briefly, mice were anesthetized, barbered on the right back, and sterilized, and then a 1-cm-by-1-cm whole-skin section was removed to make an acute skin wound according to a method described in an earlier report (49). Then, 5 μ l of 10-fold-concentrated exponential-phase *P. aeruginosa* cells (with or without CCCP or chloramphenicol pretreatment) was seeded on the wound and allowed to fully absorb before addition of 40 μ l cell-free culture medium (i.e., cells were removed by centrifugation) containing 50 or 100 μ g/ml tobramycin. After full drying, mice were locally frozen at the wound site by using liquid nitrogen-absorbed medical cotton and then the wound site was bandaged firmly with medical gauze. After mice were housed overnight, the whole scab on the wound site was removed and homogenized, with the lysates being spot plated on LB agar dishes for bacterial survival assay. For quantification, each sample was spot plated in triplicate.

Ethics statement. The animal use protocol was approved by the Animal Ethical and Welfare Committee of Fujian Normal University (approval no. IACUC 20190006), and the animal experiments were performed in accordance with the National Standards of the People's Republic of China (GB/T 35892-2018, laboratory animals—guideline for ethical review of animal welfare; GB/T 35823-2018, laboratory animals—general requirements for animal experiment).

Complementary expression of mechanosensitive ion channels. pCA24N plasmids for use in expressing the MscL, MscS, MscK, and YbdG channels were picked from the ASKA library (81), and the chloramphenicol-resistant gene in pCA24N was replaced by the ampicillin-resistant gene (as cloned from the pBAD plasmid), with the new plasmid being designated pCA24NA. *E. coli* strain MJF612 was transformed with these plasmids, cultured in LB medium to an OD₆₀₀ of 0.6, and induced to express ion channels by incubation with 0.5 mM isopropyl β -D-1-thiogalactopyranoside (IPTG) for 1 h before being subjected to the combined treatment of streptomycin plus freezing as described above. In particular, the complementary expression of MscL was induced with elevated concentrations of IPTG (1 μ M, 5 μ M, 10 μ M, and 1 mM).

Detection of endogenously expressed MscL in *E. coli* cells. To detect the endogenously expressed MscL protein in *E. coli* BW25113 cells, the *mscL* gene in the genome was modified by the use of a CRISPR-Cas system according to a method described in an earlier report (82) using GAACGTGGTGATT TGGCGG as the N20 primer. At the end, a segment of DNA sequence (GGCAGCGCCTGAACGATATTT TGAAGCGCAGAAAATTGAATGGCATGAA) was inserted into the *mscL* gene before the TAA stop codon such that an Avi tag was added to the C-terminal end of the MscL protein, and the resulting strain was named BW25113-MscL_{avi}. This strain was cultured in LB medium, NaCl-free LB medium, M9 medium plus 5 g/liter glucose medium or MHB medium. In addition, nutrient shift-induced and starvation-induced persisters were prepared as we previously described (41) and then treated with osmotic shock for 10 min using 1.25 M sucrose. All these cells were adjusted to an OD₆₀₀ of 0.6 and then subjected to the combined treatment with 25 μ g/ml tobramycin plus freezing in -80° C ethanol twice before cell survival assay. Meanwhile, cell lysates were separated with SDS gel and the Avi-tagged MscL protein was probed

by the use of alkaline phosphatase-conjugated streptavidin (which binds to the biotin attached to the Avi tag).

Statistics. CFU from LB agar dishes were counted during cell survival assays, and cell density was calculated according to the dilution fold and the volume of the cell droplet. Error bars, as calculated by the use of Microsoft Excel, represent means \pm standard deviations (SD) of results from triplicate samples. At least two independent experiments were performed for all experiments. A statistical analysis was performed using MicroOrigin software with the analysis of variance (ANOVA) algorithm at a significance level of 0.05.

SUPPLEMENTAL MATERIAL

Supplemental material is available online only.

FIG S1, PDF file, 0.2 MB.

FIG S2, PDF file, 0.2 MB.

FIG S3, PDF file, 0.5 MB.

FIG S4, PDF file, 0.5 MB.

FIG S5, PDF file, 0.3 MB.

FIG S6, PDF file, 0.5 MB.

FIG S7, PDF file, 0.5 MB.

FIG S8, PDF file, 0.6 MB.

FIG S9, PDF file, 0.3 MB.

TABLE S1, DOCX file, 0.01 MB.

ACKNOWLEDGMENTS

We thank the Nara Institute of Science and Technology (Ikoma, Nara, Japan) for providing the Keio collection and ASKA library. We appreciate Luhua Lai and Xiaoyun Liu (both of Peking University), Xuanxian Peng (Sun Yat-Sen University), and Paul Blount (University of Texas Southwestern Medical Center), as well as Qingeng Huang (Fujian Normal University) and Zhexion Tian (Peking University), for their collaboration in providing bacterial strains as described in Table S1A. We also thank Shitang Huang (Peking University) for his assistance in the radioactivity assay and Yajuan Fu (Fujian Normal University) for her assistance in flow cytometric analysis.

This work was supported by research grants from the National Natural Science Foundation of China (no. 31972918, 31770830, and 31570778 to X.F.), the Natural Science Foundation of Fujian Province (no. 2018J01725 to X.F.), and the Scientific Research Innovation Team Construction Program of Fujian Normal University (Z1707219021).

X.F. designed research; Y.Z., B.L., F.S., and J.L. performed research; X.F., Y.W., and Y.G. analyzed data; X.F. drafted the manuscript; and Z.C. revised it.

We declare that we have no conflicts of interest.

REFERENCES

- Nikaido H. 1994. Prevention of drug access to bacterial targets: permeability barriers and active efflux. *Science* 264:382–388. <https://doi.org/10.1126/science.8153625>.
- Coates A, Hu Y, Bax R, Page C. 2002. The future challenges facing the development of new antimicrobial drugs. *Nat Rev Drug Discov* 1:895–910. <https://doi.org/10.1038/nrd940>.
- Pu Y, Zhao Z, Li Y, Zou J, Ma Q, Zhao Y, Ke Y, Zhu Y, Chen H, Baker MAB, Ge H, Sun Y, Xie XS, Bai F. 2016. Enhanced efflux activity facilitates drug tolerance in dormant bacterial cells. *Mol Cell* 62:284–294. <https://doi.org/10.1016/j.molcel.2016.03.035>.
- Balaban NQ, Helaine S, Lewis K, Ackermann M, Aldridge B, Andersson DI, Brynildsen MP, Bumann D, Camilli A, Collins JJ, Dehio C, Fortune S, Ghigo JM, Hardt WT, Harms A, Heinemann M, Hung DT, Jenal U, Levin BR, Michiels J, Storz G, Tan MW, Tenson T, Van Melderen L, Zinkernagel A. 12 April 2019, posting date. Definitions and guidelines for research on antibiotic persistence. *Nat Rev Microbiol* <https://doi.org/10.1038/s41579-019-0207-4>.
- Lewis K. 2010. Persister cells. *Annu Rev Microbiol* 64:357–372. <https://doi.org/10.1146/annurev.micro.112408.134306>.
- Pu Y, Li Y, Jin X, Tian T, Ma Q, Zhao Z, Lin S-Y, Chen Z, Li B, Yao G, Leake MC, Lo C-J, Bai F. 2019. ATP-dependent dynamic protein aggregation regulates bacterial dormancy depth critical for antibiotic tolerance. *Mol Cell* 73:143–156.e144. <https://doi.org/10.1016/j.molcel.2018.10.022>.
- Lewis K. 2007. Persister cells, dormancy and infectious disease. *Nat Rev Microbiol* 5:48–56. <https://doi.org/10.1038/nrmicro1557>.
- Brauner A, Fridman O, Gefen O, Balaban NQ. 2016. Distinguishing between resistance, tolerance and persistence to antibiotic treatment. *Nat Rev Microbiol* 14:320–330. <https://doi.org/10.1038/nrmicro.2016.34>.
- Maisonneuve E, Gerdes K. 2014. Molecular mechanisms underlying bacterial persisters. *Cell* 157:539–548. <https://doi.org/10.1016/j.cell.2014.02.050>.
- Levin-Reisman I, Ronin I, Gefen O, Braniss I, Shoshitashvili N, Balaban NQ. 2017. Antibiotic tolerance facilitates the evolution of resistance. *Science* 355:826–830. <https://doi.org/10.1126/science.aaj2191>.
- Balaban NQ, Gerdes K, Lewis K, McKinney JD. 2013. A problem of persistence: still more questions than answers? *Nat Rev Microbiol* 11:587–591. <https://doi.org/10.1038/nrmicro3076>.
- O'Neill J. 2016. Tackling drug-resistant infections globally: final report and recommendations. https://amr-review.org/sites/default/files/160525_Final%20paper_with%20cover.pdf.
- WHO. 2015. Global action plan on antimicrobial resistance. World Health Organization, Geneva, Switzerland.

14. WHO. 2014. Antimicrobial resistance global report on surveillance. World Health Organization, Geneva, Switzerland.
15. Silver LL. 2011. Challenges of antibacterial discovery. *Clin Microbiol Rev* 24:71–109. <https://doi.org/10.1128/CMR.00030-10>.
16. CDC. 2013. Antibiotic resistance threats in the United States. Centers for Disease Control and Prevention, Atlanta, GA.
17. Levy SB, Marshall B. 2004. Antibacterial resistance worldwide: causes, challenges and responses. *Nat Med* 10:1222–1229. <https://doi.org/10.1038/nm1145>.
18. Allison KR, Brynildsen MP, Collins JJ. 2011. Metabolite-enabled eradication of bacterial persisters by aminoglycosides. *Nature* 473:216–220. <https://doi.org/10.1038/nature10069>.
19. Peng B, Su Y-B, Li H, Han Y, Guo C, Tian Y-M, Peng X-X. 2015. Exogenous alanine and/or glucose plus kanamycin kills antibiotic-resistant bacteria. *Cell Metab* 21:249–261. <https://doi.org/10.1016/j.cmet.2015.01.008>.
20. Su Y-B, Peng B, Li H, Cheng Z-X, Zhang T-T, Zhu J-X, Li D, Li M-Y, Ye J-Z, Du C-C, Zhang S, Zhao X-L, Yang M-J, Peng X-X. 2018. Pyruvate cycle increases aminoglycoside efficacy and provides respiratory energy in bacteria. *Proc Natl Acad Sci U S A* 115:E1578–E1587. <https://doi.org/10.1073/pnas.1714645115>.
21. Barraud N, Buson A, Jarolimek W, Rice SA. 2013. Mannitol enhances antibiotic sensitivity of persister bacteria in *Pseudomonas aeruginosa* biofilms. *PLoS One* 8:e84220. <https://doi.org/10.1371/journal.pone.0084220>.
22. Meylan S, Porter CBM, Yang JH, Belenky P, Gutierrez A, Lobritz MA, Park J, Kim SH, Moskowitz SM, Collins JJ. 2017. Carbon sources tune antibiotic susceptibility in *Pseudomonas aeruginosa* via tricarboxylic acid cycle control. *Cell Chem Biol* 24:195–206. <https://doi.org/10.1016/j.chembiol.2016.12.015>.
23. Li XZ, Nikaido H. 2009. Efflux-mediated drug resistance in bacteria: an update. *Drugs* 69:1555–1623. <https://doi.org/10.2165/11317030-000000000-00000>.
24. Mahamoud A, Chevalier J, Alibert-Franco S, Kern WV, Pagès J-M. 2007. Antibiotic efflux pumps in Gram-negative bacteria: the inhibitor response strategy. *J Antimicrob Chemother* 59:1223–1229. <https://doi.org/10.1093/jac/dkl493>.
25. Jiafeng L, Fu X, Chang Z. 2015. Hypoionic shock treatment enables aminoglycosides antibiotics to eradicate bacterial persisters. *Sci Rep* 5:14247. <https://doi.org/10.1038/srep14247>.
26. Moreau-Marquis S, O'Toole GA, Stanton BA. 2009. Tobramycin and FDA-approved iron chelators eliminate *Pseudomonas aeruginosa* biofilms on cystic fibrosis cells. *Am J Respir Cell Mol Biol* 41:305–313. <https://doi.org/10.1165/rcmb.2008-0299OC>.
27. Yu Q, Griffin EF, Moreau-Marquis S, Schwartzman JD, Stanton BA, O'Toole GA. 2012. In vitro evaluation of tobramycin and aztreonam versus *Pseudomonas aeruginosa* biofilms on cystic fibrosis-derived human airway epithelial cells. *J Antimicrob Chemother* 67:2673–2681. <https://doi.org/10.1093/jac/dks296>.
28. Uppu DSSM, Konai MM, Sarkar P, Samaddar S, Fensterseifer ICM, Farias-Junior C, Krishnamoorthy P, Shome BR, Franco OL, Halder J. 2017. Membrane-active macromolecules kill antibiotic-tolerant bacteria and potentiate antibiotics towards Gram-negative bacteria. *PLoS One* 12: e0183263. <https://doi.org/10.1371/journal.pone.0183263>.
29. Lebeaux D, Chauhan A, Létoffé S, Fischer F, de Reuse H, Beloin C, Ghigo J-M. 2014. pH-mediated potentiation of aminoglycosides kills bacterial persisters and eradicates in vivo biofilms. *J Infect Dis* 210:1357–1366. <https://doi.org/10.1093/infdis/jiu286>.
30. Falghoush A, Beyenal H, Besser TE, Omsland A, Call DR. 15 September 2017, posting date. Osmotic compounds enhance antibiotic efficacy against *Acinetobacter baumannii* biofilm communities. *Appl Environ Microbiol* <https://doi.org/10.1128/AEM.01297-17>.
31. Fridman O, Goldberg A, Ronin I, Shores N, Balaban NQ. 2014. Optimization of lag time underlies antibiotic tolerance in evolved bacterial populations. *Nature* 513:418–421. <https://doi.org/10.1038/nature13469>.
32. Keren I, Kaldalu N, Spoering A, Wang Y, Lewis K. 2004. Persister cells and tolerance to antimicrobials. *FEMS Microbiol Lett* 230:13–18. [https://doi.org/10.1016/S0378-1097\(03\)00856-5](https://doi.org/10.1016/S0378-1097(03)00856-5).
33. Balaban NQ, Merrin J, Chait R, Kowalik L, Leibler S. 2004. Bacterial persistence as a phenotypic switch. *Science* 305:1622–1625. <https://doi.org/10.1126/science.1099390>.
34. Wiuff C, Zappala RM, Regoes RR, Garner KN, Baquero F, Levin BR. 2005. Phenotypic tolerance: antibiotic enrichment of noninherited resistance in bacterial populations. *Antimicrob Agents Chemother* 49:1483–1494. <https://doi.org/10.1128/AAC.49.4.1483-1494.2005>.
35. Kwan BW, Valenta JA, Benedik MJ, Wood TK. 2013. Arrested protein synthesis increases persister-like cell formation. *Antimicrob Agents Chemother* 57:1468–1473. <https://doi.org/10.1128/AAC.02135-12>.
36. Grassi L, Di Luca M, Maisetta G, Rinaldi AC, Esin S, Trampuz A, Batoni G. 2017. Generation of persister cells of *Pseudomonas aeruginosa* and *Staphylococcus aureus* by chemical treatment and evaluation of their susceptibility to membrane-targeting agents. *Front Microbiol* 8:1917. <https://doi.org/10.3389/fmicb.2017.01917>.
37. Leviton IM, Fraimow HS, Carrasco N, Dougherty TJ, Miller MH. 1995. Tobramycin uptake in *Escherichia coli* membrane vesicles. *Antimicrob Agents Chemother* 39:467–475. <https://doi.org/10.1128/aac.39.2.467>.
38. Taber HW, Mueller JP, Miller PF, Arrow AS. 1987. Bacterial uptake of aminoglycoside antibiotics. *Microbiol Rev* 51:439–457.
39. Lobritz MA, Belenky P, Porter CBM, Gutierrez A, Yang JH, Schwarz EG, Dwyer DJ, Khalil AS, Collins JJ. 2015. Antibiotic efficacy is linked to bacterial cellular respiration. *Proc Natl Acad Sci U S A* 112:8173–8180. <https://doi.org/10.1073/pnas.1509743112>.
40. Nichols WW, Young SN. 1985. Respiration-dependent uptake of dihydrostreptomycin by *Escherichia coli*. Its irreversible nature and lack of evidence for a uniport process. *Biochem J* 228:505–512. <https://doi.org/10.1042/bj2280505>.
41. Chen Z, Gao Y, Lv B, Sun F, Yao W, Wang Y, Fu X. 2019. Hypoionic shock facilitates aminoglycoside killing of both nutrient shift- and starvation-induced bacterial persister cells by rapidly enhancing aminoglycoside uptake. *Front Microbiol* 10:2028. <https://doi.org/10.3389/fmicb.2019.02028>.
42. Mulcahy LR, Burns JL, Lory S, Lewis K. 2010. Emergence of *Pseudomonas aeruginosa* strains producing high levels of persister cells in patients with cystic fibrosis. *J Bacteriol* 192:6191–6199. <https://doi.org/10.1128/JB.01651-09>.
43. Andrews MD. 2004. Cryosurgery for common skin conditions. *Am Fam Physician* 69:2365–2372.
44. Gage AA, Baust JG. 2004. Cryosurgery for tumors - a clinical overview. *Technol Cancer Res Treat* 3:187–199. <https://doi.org/10.1177/153303460400300212>.
45. Kuflik EG. 2004. Cryosurgery for skin cancer: 30-year experience and cure rates. *Dermatol Surg* 30:297–300. <https://doi.org/10.1111/j.1524-4725.2004.30090.x>.
46. National Cancer Institute. 2017. Cryosurgery in cancer treatment. <https://www.cancer.gov/about-cancer/treatment/types/surgery/cryosurgery-fact-sheet>.
47. Pegg DE. 1987. Mechanisms of freezing damage. *Symp Soc Exp Biol* 41:363–378.
48. Mazur P. 1984. Freezing of living cells: mechanisms and implications. *Am J Physiol* 247:C125–C142. <https://doi.org/10.1152/ajpcell.1984.247.3.C125>.
49. Davidson JM. 1998. Animal models for wound repair. *Arch Dermatol Res* 290(Suppl):S1–S11. <https://doi.org/10.1007/PL00007448>.
50. Karlsson JM, Cravalho EG, Toner M. 1994. A model of diffusion-limited ice growth inside biological cell during freezing. *J Appl Phys* 75:4442–4452. <https://doi.org/10.1063/1.355959>.
51. Pegg DE. 2010. The relevance of ice crystal formation for the cryopreservation of tissues and organs. *Cryobiology* 60:536–544. <https://doi.org/10.1016/j.cryobiol.2010.02.003>.
52. Gao D, Critser JK. 2000. Mechanisms of cryoinjury in living cells. *ILAR J* 41:187–196. <https://doi.org/10.1093/ilar.41.4.187>.
53. Mazur P. 1970. Cryobiology: the freezing of biological systems. *Science* 168:939–949. <https://doi.org/10.1126/science.168.3934.939>.
54. Yu G, Yap YR, Pollock K, Hubel A. 2017. Characterizing intracellular ice formation of lymphoblasts using low-temperature Raman spectroscopy. *Biophys J* 112:2653–2663. <https://doi.org/10.1016/j.bpj.2017.05.009>.
55. Loh B, Grant C, Hancock RE. 1984. Use of the fluorescent probe 1-N-phenyl-naphthylamine to study the interactions of aminoglycoside antibiotics with the outer membrane of *Pseudomonas aeruginosa*. *Antimicrob Agents Chemother* 26:546–551. <https://doi.org/10.1128/aac.26.4.546>.
56. Daw A, Farrant J, Morris GJ. 1973. Membrane leakage of solutes after thermal shock or freezing. *Cryobiology* 10:126–133. [https://doi.org/10.1016/0011-2240\(73\)90018-7](https://doi.org/10.1016/0011-2240(73)90018-7).
57. Thalhammer A, Hinch DK, Zuther E. 2014. Measuring freezing tolerance: electrolyte leakage and chlorophyll fluorescence assays. *Methods Mol Biol* 1166:15–24. https://doi.org/10.1007/978-1-4939-0844-8_3.
58. Holt WV, Head MF, North RD. 1992. Freeze-induced membrane damage in ram spermatozoa is manifested after thawing: observations with experimental cryomicroscopy. *Biol Reprod* 46:1086–1094. <https://doi.org/10.1095/biolreprod46.6.1086>.
59. Huang Z, Lv H, Ai Z, Wang N, Xie X, Fan H, Pan Z, Suo B. 2015. Repair

- mechanism of frozen sublethally damaged *Staphylococcus aureus*. *Wei Sheng Wu Xue Bao* 55:1409–1417. (In Chinese.)
60. Sträuber H, Müller S. 2010. Viability states of bacteria-specific mechanisms of selected probes. *Cytometry A* 77:623–634.
 61. Baba T, Ara T, Hasegawa M, Takai Y, Okumura Y, Baba M, Datsenko KA, Tomita M, Wanner BL, Mori H. 2006. Construction of *Escherichia coli* K-12 in-frame, single-gene knockout mutants: the Keio collection. *Mol Syst Biol* 2:2006.0008. <https://doi.org/10.1038/msb4100050>.
 62. Iscla I, Wray R, Wei S, Posner B, Blount P. 2014. Streptomycin potency is dependent on MscL channel expression. *Nat Commun* 5:4891. <https://doi.org/10.1038/ncomms5891>.
 63. Wray R, Iscla I, Gao Y, Li H, Wang J, Blount P. 2016. Dihydrostreptomycin directly binds to, modulates, and passes through the MscL channel pore. *PLoS Biol* 14:e1002473. <https://doi.org/10.1371/journal.pbio.1002473>.
 64. Booth IR, Miller S, Muller A, Lehtovirta-Morley L. 2015. The evolution of bacterial mechanosensitive channels. *Cell Calcium* 57:140–150. <https://doi.org/10.1016/j.ceca.2014.12.011>.
 65. Schumann U, Edwards MD, Rasmussen T, Bartlett W, van West P, Booth IR. 2010. YbdG in *Escherichia coli* is a threshold-setting mechanosensitive channel with MscM activity. *Proc Natl Acad Sci U S A* 107:12664–12669. <https://doi.org/10.1073/pnas.1001405107>.
 66. Davis BD, Chen LL, Tai PC. 1986. Misread protein creates membrane channels: an essential step in the bactericidal action of aminoglycosides. *Proc Natl Acad Sci U S A* 83:6164–6168. <https://doi.org/10.1073/pnas.83.16.6164>.
 67. Davis BD. 1987. Mechanism of bactericidal action of aminoglycosides. *Microbiol Rev* 51:341–350.
 68. Ling J, Cho C, Guo L-T, Aerni HR, Rinehart J, Söll D. 2012. Protein aggregation caused by aminoglycoside action is prevented by a hydrogen peroxide scavenger. *Mol Cell* 48:713–722. <https://doi.org/10.1016/j.molcel.2012.10.001>.
 69. Fraimow HS, Greenman JB, Leviton IM, Dougherty TJ, Miller MH. 1991. Tobramycin uptake in *Escherichia coli* is driven by either electrical potential or ATP. *J Bacteriol* 173:2800–2808. <https://doi.org/10.1128/jb.173.9.2800-2808.1991>.
 70. Bank H, Mazur P. 1973. Visualization of freezing damage. *J Cell Biol* 57:729–742. <https://doi.org/10.1083/jcb.57.3.729>.
 71. Ray B, Speck ML. 1973. Freeze-injury in bacteria. *CRC Crit Rev Clin Lab Sci* 4:161–213. <https://doi.org/10.3109/10408367309151556>.
 72. Booth IR. 2014. Bacterial mechanosensitive channels: progress towards an understanding of their roles in cell physiology. *Curr Opin Microbiol* 18:16–22. <https://doi.org/10.1016/j.mib.2014.01.005>.
 73. Iscla I, Blount P. 2012. Sensing and responding to membrane tension: the bacterial MscL channel as a model system. *Biophys J* 103:169–174. <https://doi.org/10.1016/j.bpj.2012.06.021>.
 74. Haswell ES, Phillips R, Rees DC. 2011. Mechanosensitive channels: what can they do and how do they do it? *Structure* 19:1356–1369. <https://doi.org/10.1016/j.str.2011.09.005>.
 75. Bachin D, Nazarenko LV, Mironov KS, Pisareva T, Allakhverdiev SI, Los DA. 2015. Mechanosensitive ion channel MscL controls ionic fluxes during cold and heat stress in *Synechocystis*. *FEMS Microbiol Lett* 362:fnv090. <https://doi.org/10.1093/femsle/fnv090>.
 76. Nazarenko LV, Andreev IM, Lyukevich AA, Pisareva TV, Los DA. 2003. Calcium release from *Synechocystis* cells induced by depolarization of the plasma membrane: MscL as an outward Ca²⁺ channel. *Microbiology* 149:1147–1153. <https://doi.org/10.1099/mic.0.26074-0>.
 77. Sukharev SI, Martinac B, Arshavsky VY, Kung C. 1993. Two types of mechanosensitive channels in the *Escherichia coli* cell envelope: solubilization and functional reconstitution. *Biophys J* 65:177–183. [https://doi.org/10.1016/S0006-3495\(93\)81044-0](https://doi.org/10.1016/S0006-3495(93)81044-0).
 78. Wray R, Herrera N, Iscla I, Wang J, Blount P. 2019. An agonist of the MscL channel affects multiple bacterial species and increases membrane permeability and potency of common antibiotics. *Mol Microbiol* 112:896–905. <https://doi.org/10.1111/mmi.14325>.
 79. Fu X, Wang P, Zhu BT. 2008. Protein disulfide isomerase is a multifunctional regulator of estrogenic status in target cells. *J Steroid Biochem Mol Biol* 112:127–137. <https://doi.org/10.1016/j.jsbmb.2008.09.005>.
 80. Ge X, Wang R, Ma J, Liu Y, Ezemaduka AN, Chen PR, Fu X, Chang Z. 2014. DegP primarily functions as a protease for the biogenesis of beta-barrel outer membrane proteins in the Gram-negative bacterium *Escherichia coli*. *FEBS J* 281:1226–1240. <https://doi.org/10.1111/febs.12701>.
 81. Kitagawa M, Ara T, Arifuzzaman M, Ioka-Nakamichi T, Inamoto E, Toyonaga H, Mori H. 2005. Complete set of ORF clones of *Escherichia coli* ASKA library (a complete set of *E. coli* K-12 ORF archive): unique resources for biological research. *DNA Res* 12:291–299. <https://doi.org/10.1093/dnares/dsi012>.
 82. Jiang Y, Chen B, Duan C, Sun B, Yang J, Yang S. 2015. Multigene editing in the *Escherichia coli* genome via the CRISPR-Cas9 system. *Appl Environ Microbiol* 81:2506–2514. <https://doi.org/10.1128/AEM.04023-14>.